

The GGCMI Phase II experiment: global crop yield responses to changes in carbon dioxide, temperature, water, and nitrogen levels

James Franke^{a,b,*}, Joshua Elliott^{b,c}, Christoph Müller^d, Alexander Ruane^e, Abigail Snyder^f, Jonas Jägermeyr^{c,b,d,e}, Juraj Balkovic^{g,h}, Philippe Ciais^{i,j}, Marie Dury^k, Pete Falloon^l, Christian Folberth^g, Louis François^k, Tobias Hank^m, Munir Hoffmannⁿ, Cesar Izaurralde^{o,p}, Ingrid Jacquemin^k, Curtis Jones^o, Nikolay Khabarov^g, Marian Kochⁿ, Michelle Li^{b,l}, Wenfeng Liu^{r,i}, Stefan Olin^s, Meridel Phillips^{e,t}, Thomas Pugh^{u,v}, Ashwan Reddy^o, Xuhui Wang^{i,j}, Karina Williams^l, Florian Zabel^m, Elisabeth Moyer^{a,b}

^aDepartment of the Geophysical Sciences, University of Chicago, Chicago, IL, USA

^bCenter for Robust Decision-making on Climate and Energy Policy (RDCEP), University of Chicago, Chicago, IL, USA

^cDepartment of Computer Science, University of Chicago, Chicago, IL, USA

^dPotsdam Institute for Climate Impact Research, Leibniz Association (Member), Potsdam, Germany

^eNASA Goddard Institute for Space Studies, New York, NY, United States

^fJoint Global Change Research Institute, Pacific Northwest National Laboratory, College Park, MD, USA

^gEcosystem Services and Management Program, International Institute for Applied Systems Analysis, Laxenburg, Austria

^hDepartment of Soil Science, Faculty of Natural Sciences, Comenius University in Bratislava, Bratislava, Slovak Republic

ⁱLaboratoire des Sciences du Climat et de l'Environnement, CEA-CNRS-UVSQ, 91191 Gif-sur-Yvette, France

^jSino-French Institute of Earth System Sciences, College of Urban and Environmental Sciences, Peking University, Beijing, China

^kUnité de Modélisation du Climat et des Cycles Biogéochimiques, UR SPHERES, Institut d'Astrophysique et de Géophysique, University of Liège, Belgium

^lMet Office Hadley Centre, Exeter, United Kingdom

^mDepartment of Geography, Ludwig-Maximilians-Universität, Munich, Germany

ⁿGeorg-August-University Göttingen, Tropical Plant Production and Agricultural Systems Modelling, Göttingen, Germany

^oDepartment of Geographical Sciences, University of Maryland, College Park, MD, USA

^pTexas AgriLife Research and Extension, Texas A&M University, Temple, TX, USA

^qDepartment of Statistics, University of Chicago, Chicago, IL, USA

^rEAWAG, Swiss Federal Institute of Aquatic Science and Technology, Dübendorf, Switzerland

^sDepartment of Physical Geography and Ecosystem Science, Lund University, Lund, Sweden

^tEarth Institute Center for Climate Systems Research, Columbia University, New York, NY, USA

^uKarlsruhe Institute of Technology, IMK-IFU, 82467 Garmisch-Partenkirchen, Germany.

^vSchool of Geography, Earth and Environmental Science, University of Birmingham, Birmingham, UK.

Abstract

Concerns about food security under climate change have motivated efforts to better understand the future changes in yields by using detailed process-based models in agronomic sciences. Process-based models differ on many details affecting yields and considerable uncertainty remains in future yield projections. Phase II of the Global Gridded Crop Model Intercomparison (GGCMI), an activity of the Agricultural Model Intercomparison and Improvement Project (AgMIP), consists of a large simulation set with perturbations in atmospheric CO₂ concentrations, temperature, precipitation, and nitrogen inputs and constitutes a data-rich basis of projected yield changes across 12 models and five crops (maize, soy, rice, spring wheat, and winter wheat) using global gridded simulations for twelve different process-based models. In this paper we present the simulation output database from Phase II of the GGCMI effort, a targeted experiment aimed at understanding the sensitivity to and interaction between multiple climate variables (as well as management) on yields, and illustrate some initial summary results from the model intercomparison project. We also present the construction of a simple “emulator or statistical representation of the simulated 30-year mean climatological output in each location for each crop and model. The emulator captures the response of the process-based models in a lightweight, computationally tractable form that facilitates model comparison as well as potential applications in subsequent modeling efforts such as integrated assessment.

Keywords: climate change, food security, model emulation, AgMIP, crop model

1. Introduction

2 Projecting crop yield response to a changing climate is of
3 great importance, especially as the global food production sys-
4 tem will face pressure from increased demand over the next
5 century. Climate-related reductions in supply could therefore
6 have severe socioeconomic consequences. Multiple studies
7 with different crop or climate models predict sharp reduction in
8 yields on currently cultivated cropland under business-as-usual
9 climate scenarios, although their yield projections show consid-
10 erable spread (e.g. Porter et al. (IPCC), 2014, Rosenzweig et al.,
11 2014, Schauberger et al., 2017, and references therein). Model
12 differences are unsurprising because crop responses in models
13 can be complex, with crop growth a function of complex inter-
14 actions between climate inputs and management practices.

15 Computational Models have been used to project crop yields
16 since the 1950's, beginning with statistical models (Heady,
17 1957, Heady & Dillon, 1961) that attempt to capture the rela-
18 tionship between input factors and resultant yields. These sta-
19 tistical models were typically developed on a small scale for lo-
20 cations with extensive histories of yield data. The emergence of
21 computers allowed development of numerical models that sim-
22 ulate the process of photosynthesis and the biology and phe-
23 nology of individual crops (first proposed by de Wit (1957),
24 Duncan et al. (1967) and attempted by Duncan (1972)). His-
25 torical mapping of crop model development can be found in
26 the appendix/supplementary of Rosenzweig et al. (2014). A
27 half-century of improvement in both models and computing re-
28 sources means that researchers can now run crop simulation
29 models for many years at high spatial resolution on the global
30 scale.

31 Both types of models continue to be used, and compara-
32 tive studies have concluded that when done carefully, both ap-

33 proaches can provide similar yield estimates (e.g. Lobell &
34 Burke, 2010, Moore et al., 2017, Roberts et al., 2017, Zhao
35 et al., 2017). Models tend to agree broadly in major response
36 patterns, including a reasonable representation of the spatial
37 pattern in historical yields of major crops (e.g. Elliott et al.,
38 2015, Müller et al., 2017) and projections of decreases in yield
39 under future climate scenarios.

40 Process models do continue to struggle with some important
41 details, including reproducing historical year-to-year variabil-
42 ity (e.g. Müller et al., 2017), reproducing historical yields when
43 driven by reanalysis weather (e.g. Glotter et al., 2014), and low
44 sensitivity to extreme events (e.g. Glotter et al., 2015). These
45 issues are driven in part by the diversity of new cultivars and ge-
46 netic variants, which outstrips the ability of academic modeling
47 groups to capture them (e.g. Jones et al., 2017). Models do not
48 simulate many additional factors affecting production, includ-
49 ing pests/diseases/weeds. For these reasons, individual stud-
50 ies must generally re-calibrate models to ensure that short-term
51 predictions reflect current cultivar mixes, and long-term pro-
52 jections retain considerable uncertainty (Wolf & Oijen, 2002,
53 Jagtap & Jones, 2002, Iizumi et al., 2010, Angulo et al., 2013,
54 Asseng et al., 2013, 2015). Inter-model discrepancies can also
55 be high in areas not yet cultivated (e.g. Challinor et al., 2014,
56 White et al., 2011). Finally, process-based models present ad-
57 dditional difficulties for high-resolution global studies because
58 of their complexity and computational requirements. For eco-
59 nomic impacts assessments, it is often impossible to integrate a
60 set of process-based crop models directly into an integrated as-
61 sessment model to estimate the potential cost of climate change
62 to the agricultural sector.

63 Nevertheless, process-based models are necessary for under-
64 standing the global future yield impacts of climate change for
65 many reasons. First, cultivation may shift to new areas, where
66 no yield data are currently available and therefore statistical

*Corresponding author at: 4734 S Ellis, Chicago, IL 60637, United States.
email: jfranke@uchicago.edu

67 models cannot apply. Yield data are also often limited in the de-
 68 veloping world, where future climate impacts may be the most
 69 critical. Second, only process-based models can capture the
 70 growth response to elevated CO₂, novel conditions that are not
 71 represented in historical data (e.g. Pugh et al., 2016, Roberts
 72 et al., 2017). Similarly process-based models can represent
 73 novel changes in management practices (e.g. fertilizer input)
 74 that may ameliorate climate-induced damages.

75 The overall goal of this study is a better understanding of
 76 global crop model response to the major drivers in a climate
 77 change context. Most previous climate-change-focused global
 78 crop modeling studies have simulated model response to rep-
 79 resentative concentration pathways (RCPs). RCPs are likely to
 80 have strong covariance between precipitation, temperature and
 81 CO₂ that may be hard to decompose statistically. The differ-
 82 ences in year-to-year memory in the models and complexity of
 83 the changes in year-to-year distributions in weather under RCP
 84 scenarios in climate models are complications we seek to con-
 85 trol for with this study. We propose to test the response to major
 86 drivers and their interaction by isolating individual input drivers
 87 through simulations on first-moment shifts applied to the histor-
 88 ical climatology instead of RCP simulations. As emulators are
 89 a fundamentally a distillation of the process-based model down
 90 to its major drivers, the same applied to their development.

91 Statistical emulation of crop simulations has been used to
 92 combine advantageous features of both statistical and process-
 93 based models. The statistical representation of complicated nu-
 94 merical simulation (e.g. O'Hagan, 2006, Conti et al., 2009), in
 95 which simulation output acts as the training data for a statisti-₁₀₁
 96 cal model, has been of increasing interest with the growth of₁₀₂
 97 simulation complexity and volume of output. Such emulators₁₀₃
 98 or "surrogate models" have been used in a variety of fields in-₁₀₄
 99 cluding hydrology (e.g. Razavi et al., 2012), engineering (e.g.₁₀₅
 100 Storlie et al., 2009), environmental sciences (e.g. Ratto et al.,₁₀₆

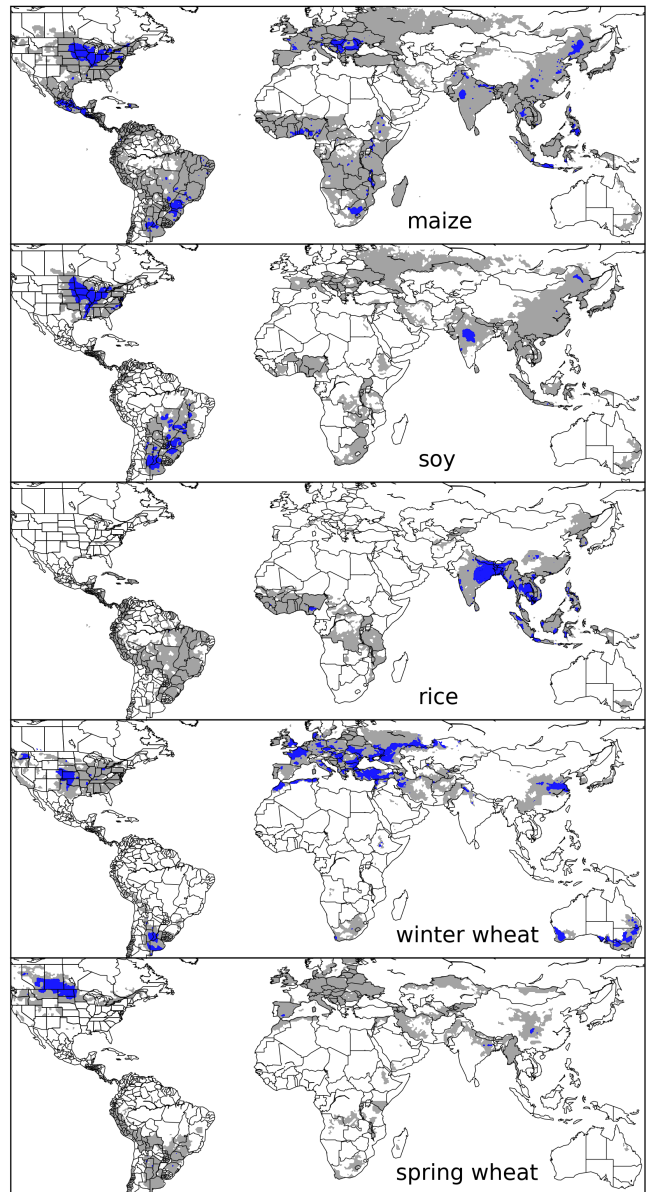


Figure 1: Presently cultivated area for rain-fed crops in the real world. Blue contour area indicates grid cells with more than 20,000 hectares (approx. 10% of the land in a grid cell near the equator for example) of crop cultivated. Gray contour shows area with more than 10 hectares cultivated. Cultivated areas for maize, rice, and soy are taken from the MIRCA2000 ("monthly irrigated and rain-fed crop areas around the year 2000") dataset (Portmann et al., 2010). Areas for winter and spring wheat areas are adapted from MIRCA2000 data and sorted by growing season. For analogous figure of irrigated crops, see Figure S1.

2012), and climate (e.g. Castruccio et al., 2014, Holden et al.,
 2014). For agricultural impacts studies, emulation of process-
 based models allows exploring crop yields in regions outside
 ranges of current cultivation and with input variables outside
 historical precedents, in a lightweight, flexible form that is com-
 patible with economic studies.

In the past decade, many studies have developed emulators of crop yields from process-based models. Early studies proposing or describing potential emulators include Howden & Crimp (2005), Räisänen & Ruokolainen (2006) and Lobell & Burke (2010). In an early application, Ferrise et al. (2011) used a Artificial Neural Net trained on simulation outputs to predict wheat yields in the Mediterranean. Studies developing single-model emulators include Holzkämper et al. (2012) for the CropSyst model, Ruane et al. (2013) for the CERES wheat model, Oyebamiji et al. (2015) for the LPJmL model (for multiple crops, using multiple scenarios as a training set). In recent years, emulators have begun to be used in the context of multi-model inter-comparisons, with Blanc & Sultan (2015), Blanc (2017), Ostberg et al. (2018) and Mistry et al. (2017) using them to analyze the five crop models of the Inter-Sectoral Impacts Model Intercomparison Project (ISIMIP) (Warszawski et al., 2014) (for maize, soy, wheat, and rice). Approaches differ: Blanc & Sultan (2015) and Blanc (2017) used local weather variables (and CO₂ values) and yields but emulate across soil types using historical simulations and a future climate scenario (RCP8.5 over multiple climate models); Ostberg et al. (2018) used global mean temperature change (and CO₂) as regressors but pattern-scale to emulate local yields using multiple climate scenarios; Mistry et al. (2017) used local weather and yields and a historical simulation and compare with data.

Recently efforts have been made to generate datasets that allow more systematic sampling of the input variable space (the focus of this study): Makowski et al. (2015) for temperature, CO₂,

and nitrogen, Pirttioja et al. (2015) and Snyder et al. (2018) for temperature, water, and CO₂, and (Fronzek et al., 2018) for temperature and water, with all studies simulating selected sites for a limited number of crops.

The use of limited input parameter space or restricted geographic scope may impede the ability to build future projections or to understand interaction effects in global process-based crop models.

The Global Gridded Crop Model Intercomparison (GGCMI) Phase II experiment seeks to provide a comprehensive global dataset to allow systematically exploring how process-based crop models for the major crop respond to the main climate and management drivers and their interactions. The experiment involves running a suite of process-based crop models across historical conditions perturbed by a set of defined input parameters, and was conducted as part of the Agricultural Model Intercomparison and Improvement Project (AgMIP) (Rosenzweig et al., 2013, 2014), an international effort conducted under a framework similar to the Climate Model Intercomparison Project (CMIP) (Taylor et al., 2012, Eyring et al., 2016). The GGCMI protocol builds on the AgMIP Coordinated Climate-Crop Modeling Project (C3MP) (Ruane et al., 2014, McDermid et al., 2015) and will contribute to the AgMIP Coordinated Global and Regional Assessments (CGRA) (Ruane et al., 2018, Rosenzweig et al., 2018).

GGCMI Phase II is designed to allow addressing goals such as understanding where highest-yield regions may shift under climate change; exploring future adaptive management

Input variable	Abbr.	Tested range	Unit
CO ₂	C	360, 510, 660, 810	ppm
Temperature	T	-1, 0, 1, 2, 3, 4, 5*, 6	°C
Precipitation	W	-50, -30, -20, -10, 0, 10, 20, 30, (and W _{inf})	%
Applied nitrogen	N	10, 60, 200	kg ha ⁻¹

Table 1: Phase II input variable test levels. Temperature and precipitation values indicate the perturbations from the historical, climatology. * Only simulated by one model. W-percentage does not apply to the irrigated (W_{inf}) simulations.

strategies; understanding how interacting parameters affect¹⁹⁵
crop yield; quantifying uncertainties across models and major¹⁹⁶
drivers; and testing strategies for producing lightweight emu-¹⁹⁷
lators of process-based models. In this paper, we describe the¹⁹⁸
GGCMI Phase II experiments, summarize output and present¹⁹⁹
initial results, demonstrate that it is tractable to emulation, and²⁰⁰
present a simple climatological emulator as a potential tool for²⁰¹
impacts assessments.²⁰²

2. Materials and Methods

2.1. GGCMI Phase II: experiment design

GGCMI Phase II is the continuation of a multi-model com-²⁰⁶
parison exercise begun in 2014. The initial Phase I compared²⁰⁷
harmonized yields of 21 models for 19 crops over a historical²⁰⁸
(1980-2010) scenario with a primary goal of model evaluation²⁰⁹
(Elliott et al., 2015, Müller et al., 2017). Phase II compares sim-²¹⁰
ulations of 12 models for 5 crops (maize, rice, soybean, spring²¹¹
wheat, and winter wheat) over hundreds of scenarios in which²¹²
individual climate or management inputs are adjusted from²¹³
their historical values. The reduced set of crops includes the²¹⁴
three major global cereals and the major legume and accounts²¹⁵
for over 50% of human calories (in 2016, nearly 3.5 billion tons²¹⁶
or 32% of total global crop production by weight (Food and²¹⁷
Agriculture Organization of the United Nations, 2018).

The major goals of GGCMI Phase II are to:

- Enhance understanding of how models work by characterizing their sensitivity to input climate and nitrogen drivers.
- Study the interactions between climate variables and nitrogen inputs in driving modeled yield impacts.
- Explore differences in crop response to warming across the Earth's climate regions.
- Provide a dataset that allows statistical emulation of crop model responses for downstream modelers.

- Illustrate differences in potential adaptation via growing season changes.

The guiding scientific rationale of GGCMI Phase II is to provide a comprehensive, systematic evaluation of the response of process-based crop models to different values for carbon dioxide, temperature, water, and applied nitrogen (collectively known as “CTWN”). Phase II of the GGCMI project consists of a series of simulations, each with one or more of the CTWN dimensions perturbed over the 31-year historical time series (1980-2010) used in Phase I. In most cases, historical daily climate inputs are taken from the 0.5 degree NASA AgMERRA daily gridded re-analysis product specifically designed for agricultural modeling, with satellite-corrected precipitation (Ruane et al., 2015). Two models require sub-daily input data and use alternative sources. See Elliott et al. (2015) for additional details.

The experimental protocol consists of 9 levels for precipitation perturbations, 7 for temperature, 4 for CO₂, and 3 for applied nitrogen, for a total of 672 simulations for rain-fed agriculture and an additional 84 for irrigated (Table 1). For irrigated simulations, soil water is held at either field capacity or, for those models that include water-log damage, at maximum beneficial level. Temperature perturbations are applied as absolute offsets from the daily mean, minimum, and maximum temperature time series for each grid cell used as inputs. Precipitation perturbations are applied as fractional changes at the grid cell level, and carbon dioxide and nitrogen levels are specified as discrete values applied uniformly over all grid cells. Note that CO₂ changes are applied independently of changes in climate variables, so that higher CO₂ is not associated with higher temperatures. An additional, identical set of scenarios (at the same C, T, W, and N levels) simulate adaptive agronomy under climate change by varying the growing season for crop production. (These adaptation simulations are not shown

Model (Key Citations)	Maize	Soy	Rice	Winter Wheat	Spring Wheat	N Dim.	Simulations per Crop
APSIM-UGOE , Keating et al. (2003), Holzworth et al. (2014)	X	X	X	–	X	Yes	37
CARAIB , Dury et al. (2011), Pirttioja et al. (2015)	X	X	X	X	X	No	224
EPIC-IIASA , Balkovi et al. (2014)	X	X	X	X	X	Yes	35
EPIC-TAMU , Izaurrealde et al. (2006)	X	X	X	X	X	Yes	672
JULES* , Osborne et al. (2015), Williams & Falloon (2015), Williams et al. (2017)	X	X	X	–	X	No	224
GEPIG , Liu et al. (2007), Folberth et al. (2012)	X	X	X	X	X	Yes	384
LPJ-GUESS , Lindeskog et al. (2013), Olin et al. (2015)	X	–	–	X	X	Yes	672
LPJmL , von Bloh et al. (2018)	X	X	X	X	X	Yes	672
ORCHIDEE-crop , Valade et al. (2014)	X	–	X	–	X	Yes	33
pDSSAT , Elliott et al. (2014), Jones et al. (2003)	X	X	X	X	X	Yes	672
PEPIC , Liu et al. (2016a,b)	X	X	X	X	X	Yes	130
PROMET*† , Mauser & Bach (2015), Hank et al. (2015), Mauser et al. (2009)	X	X	X	X	X	Yes†	239
Totals	12	10	11	9	12	–	3993 (maize)

Table 2: Models included in the GGCMI Phase II and the number of C, T, W, and N simulations performed for rain-fed crops (“Sims per Crop”), with 672 as the maximum. “N-Dim.” indicates if simulations include varying nitrogen levels; two models omit this dimension. All models provided the same set of simulations across all modeled crops, but some omitted individual crops in some cases. (For example, APSIM did not simulate winter wheat.) Irrigated simulations are provided at the level of the other covariates for each model (for an additional 84 simulations for the fully-sampled models). Geographic extent of simulation varies to some extent within a certain model for different scenarios (672 rain-fed simulations does not necessarily equal 672 climatological yields in all areas). This geographic variance only applies for areas far outside the area of currently cultivated crops. Two models (marked with *) use non-AgMERRA climate inputs. For further details on models, see Elliott et al. (2015). †PROMET provided simulations at only two nitrogen levels so is not emulated across the nitrogen dimension.

229 or analyzed here.) The resulting GGCMI data set captures a₂₄₇ such as atmospheric deposition, are considered, but some mod-
230 distribution of crop responses over the potential space of future₂₄₈ els have individual assumptions on soil organic matter that may
231 climate conditions. ₂₄₉ release additional nitrogen through mineralization. See Rosen-
232 The 12 models included in GGCMI Phase II are all mecha-₂₅₁ zweig et al. (2014), Elliott et al. (2015) and Müller et al. (2017)
233 nistic process-based crop models that are widely used in im-
234 pacts assessments (Table 2). Although some of the models₂₅₂ for further details on models and underlying assumptions.
235 shares a common base (e.g. LPJmL and LPJ-GUESS and the₂₅₃
236 EPIC models), they have developed independently from this₂₅₄
237 shared base, for more details on the genealogy of the mod-₂₅₅
238 els see Figure S1 in Rosenzweig et al. (2014). Differences in₂₅₆
239 model structure does mean that several key factors are not stan-₂₅₇
240 dardized across the experiment, including secondary soil nutri-₂₅₈
241 ents, carry over effects across growing years including residue₂₅₉
242 management and soil moisture, and extent of simulated area for₂₆₀
243 different crops. Growing seasons are identical across models,₂₆₁
244 but vary by crop and by location on the globe. All stresses₂₆₂
245 except factors related to nitrogen, temperature, and water (e.g.,₂₆₃
246 Alkalinity, salinity) are disabled. No additional nitrogen inputs,₂₆₄

Each model is run at 0.5 degree spatial resolution and covers all currently cultivated areas and much of the uncultivated land area. Coverage extends considerably outside currently cultivated areas because cultivation will likely shift under climate change. See Figure 1 for the present-day cultivated area of rain-fed crops, and Figure S1 in the supplemental material for irrigated crops. Some areas such as Greenland, far-northern Canada, Siberia, Antarctica, the Gobi and Sahara deserts, and central Australia are not simulated as they are assumed to remain non-arable even under an extreme climate change. Growing seasons are standardized across models with data adapted from several sources (Sacks et al., 2010, Portmann et al., 2008, 2010).

265 The participating modeling groups provide simulations at²⁹⁹
 266 any of four initially specified levels of participation, so the num-³⁰⁰
 267 ber of simulations varies by model, with some sampling only a³⁰¹
 268 part of the experiment variable space. Most modeling groups³⁰²
 269 simulate all five crops in the protocol, but some omitted one³⁰³
 270 or more. Table 2 provides details of coverage for each model.³⁰⁴
 271 Note that the three models that provide less than 50 simulations
 272 are excluded from the emulator analysis.³⁰⁵

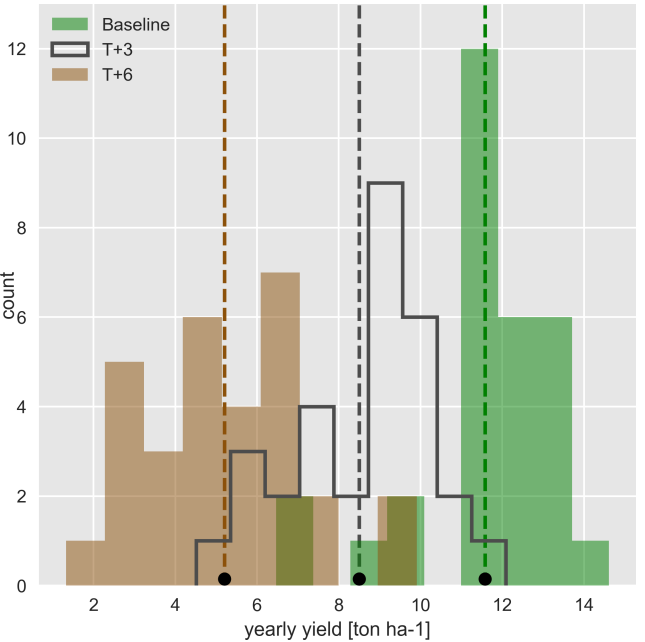
273 All models produce as output, crop yields ($\text{tons ha}^{-1} \text{ year}^{-1}$)
 274 for each 0.5 degree grid cell. Because both yields and yield
 275 changes vary substantially across models and across grid cells,
 276 we primarily analyze relative change from a baseline. We take
 277 as the baseline the scenario with historical climatology (i.e. T
 278 and P changes of 0). C of 360 ppm, and applied N at 200 kg
 279 ha^{-1} . We show absolute yields in some cases to illustrate geo-
 280 graphic differences in yields for a single model.

2.2. Simulation model validation approach

281 To verify the skill of the process-based models used, we re-
 282 peat the validation exercises presented in Müller et al. (2017)
 283 for GGCMI Phase I. Note however that the GGCMI Phase II
 284 simulations are designed for evaluating changes in yield but not
 285 absolute yields, and so omit the calibrations used in predict-
 286 ing modeling to account for cultivar, pest loss, and manage-
 287 ment differences. The Phase II simulations also do not repro-
 288 duce realistic nitrogen application levels for individual coun-³⁰⁷
 289 tries, since nitrogen is one of the parameters systematically var-³⁰⁷
 290 ied. The Müller et al. (2017) validation procedure evaluates re-³⁰⁸
 291 sponse to year-to-year temperature and precipitation variations³⁰⁹
 292 in a control run driven by historical climate and compares it³¹⁰
 293 to detrended historical yields from the FAO (Food and Agri-³¹¹
 294 culture Organization of the United Nations, 2018) by calculat-³¹²
 295 ing the Pearson correlation coefficient. The procedure offers no³¹³
 296 means of assessing CO₂ fertilization, since CO₂ has been rel-³¹⁴
 297 atively constant over the historical data collection period. Ni-³¹⁵

298 trogen data are limited for many countries, and as mentioned
 299 the GGCMI Phase II runs impose fixed and uniform nitrogen
 300 application, introducing some uncertainty into the analysis. We
 301 evaluate one or more control runs for each model, since some
 302 modeling groups provide historical runs for three different ni-
 303 tragen levels.

2.3. Climatological-mean yield emulator design



304 Figure 2: Example showing both climatological mean yields and distribution
 305 of yearly yields for three 30-year scenarios. Figure shows rain-fed maize for a
 306 grid cell in northern Iowa (a representative high-yield region) from the pDSSAT
 307 model, for the baseline climatology (1981–2010) and for scenarios with tem-
 308 perature shifted by (T) +3 and (T) +6 °C, with other variables held at baseline
 309 values. Dashed vertical lines and black dots indicate the climatological mean
 310 yield.

311 We construct our emulator at the 30-year climatological
 312 mean level. Blanc & Sultan (2015) and Blanc (2017) have
 313 shown that a emulator of a global process-based crop model can
 314 be successfully developed at the yearly scale. Our decision to
 315 construct a climatological-mean yield emulator is driven by the
 316 target application for this analysis tool. Many impact modelers
 317 are not focused on the changes in the year-to-year variability in
 318 yields, but instead on the broad mean changes over the multi-
 319 decadal timescale. Emulation involves fitting individual regres-
 320 sion models for each crop, simulation model, and 0.5 degree

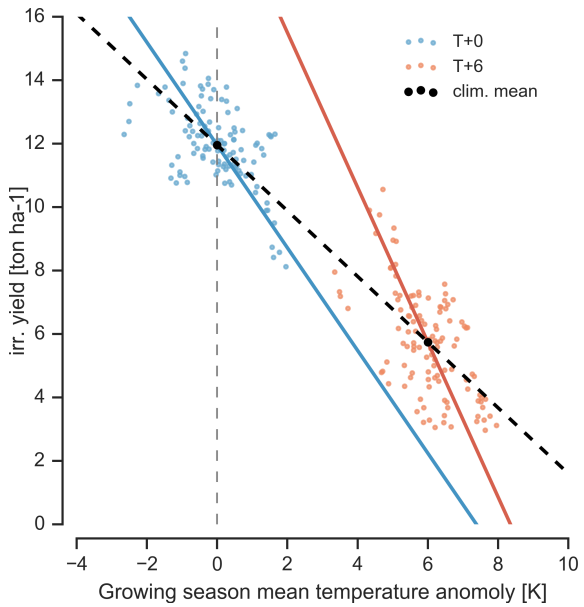


Figure 3: Example showing simple temperature relationship developed from year-to-year values vs. climatological mean values. Figure shows irrigated maize for four adjacent grid cell in northern Iowa (a representative high-yield region) from the pdSSAT model, for the baseline climatology (1981-2010) and for scenarios with temperature shifted (T) $+6^{\circ}\text{C}$, with other variables held at baseline values. Irrigated yields are shown to control for precipitation effects. Blue and red lines indicate total least squares linear regression across each temperature scenario. Black dots indicate the climatological mean yield values for each climatological temperature scenario.

Blanc & Sultan (2015) and Blanc (2017) have shown that a fractional polynomial specification is more effective than a standard polynomial for representing simulations at the yearly level across different soil types geographically (not at the grid cell level). We do not test this specification here, and instead use as a starting point a standard third-order polynomial to represent the climatological-mean response at the grid cell level as it is the simplest effective specification. We regress climatological-mean yields against a third-order polynomial in C , T , W , and N with interaction terms. The higher-order terms are necessary to capture any nonlinear responses, which are well-documented in observations for temperature and water perturbations (e.g. Schlenker & Roberts (2009) for T and He et al. (2016) for W). We include interaction terms (both linear and higher-order) because past studies have shown them to be significant effects. For example, Lobell & Field (2007) and Tebaldi & Lobell (2008) showed that in real-world yields, the joint distribution in T and W is needed to explain observed yield variance (C and N are fixed in these data). Other observation-based studies have shown the importance of the interaction between water and nitrogen (e.g. Aulakh & Malhi, 2005), and between nitrogen and carbon dioxide (Osaki et al., 1992, Nakamura et al., 1997). We do not focus on comparing different model specifications in this study, and instead stick to a relatively simple parameterized specification that allows for some, albeit limited, coefficient interpretation.

geographic pixel from the GGCMI Phase II data set. The regressors are the applied constant perturbations in temperature, water, nitrogen and CO_2 , we aggregate the simulation outputs in the time dimension, and regress on the 30-year mean yields. (See Figure 2 for illustration). The regression therefore omits information about yield responses to year-to-year climate perturbations, which are more complex. Emulating inter-annual yield variations would likely require considering statistical details of the historical climate time series, including changes in marginal distribution and temporal dependencies. (Future work should explore this). The climatological emulation indirectly includes any yield response to geographically distributed factors such as soil type, insolation, and the baseline climate itself, because we construct separate emulators for each grid cell. The emulator parameter matrices are portable and the yield computations are cheap even at the half-degree grid cell resolution, so we do not aggregate in space at this time.

The limited GGCMI variable sample space means that use of the full polynomial expression described above, which has 34 terms for the rain-fed case (12 for irrigated), can be problematic, and can lead to over-fitting and unstable parameter estimations. We therefore reduce the number of terms through a feature selection cross-validation process in which terms in the polynomial are tested for importance. In this procedure higher-order and interaction terms are added successively to the model;

we then follow the reduction of the aggregate mean squared error with increasing terms and eliminate those terms that do not contribute significant reductions. See supplemental documents for more details. We select terms by applying the feature selection process to the three models that provided the complete set of 672 rain-fed simulations (pDSSAT, EPIC-TAMU, and LPJmL); the resulting choice of terms is then applied for all emulators.

Feature importance is remarkably consistent across all three models and across all crops (see Figure S4 in the supplemental material). The feature selection process results in a final polynomial in 23 terms, with 11 terms eliminated. We omit the N^3 term, which cannot be fitted because we sample only three nitrogen levels. We eliminate many of the C terms: the cubic, the CT, CTN, and CWN interaction terms, and all higher order interaction terms in C. Finally, we eliminate two 2nd-order interaction terms in T and one in W. Implication of this choice

include that nitrogen interactions are complex and important, and that water interaction effects are more nonlinear than those in temperature. The resulting statistical model (Equation 1) is used for all grid cells, models, and crops:

$$\begin{aligned}
 Y &= K_1 \\
 &+ K_2 C + K_3 T + K_4 W + K_5 N \\
 &+ K_6 C^2 + K_7 T^2 + K_8 W^2 + K_9 N^2 \\
 &+ K_{10} CW + K_{11} CN + K_{12} TW + K_{13} TN + K_{14} WN \\
 &+ K_{15} T^3 + K_{16} W^3 + K_{17} TWN \\
 &+ K_{18} T^2 W + K_{19} W^2 T + K_{20} W^2 N \\
 &+ K_{21} N^2 C + K_{22} N^2 T + K_{23} N^2 W
 \end{aligned} \tag{1}$$

To fit the parameters K , we use a Bayesian Ridge probabilistic estimator (MacKay, 1991), which reduces volatility in parameter estimates when the sampling is sparse, by weighting

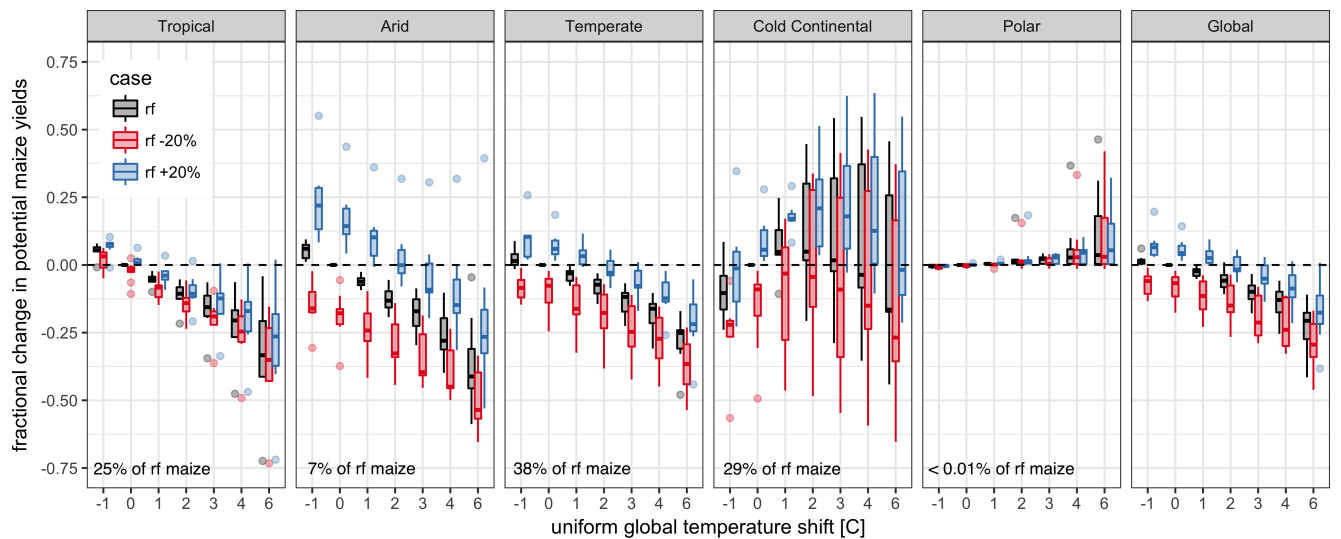


Figure 4: Illustration of the distribution of regional yield changes across the multi-model ensemble, split by Köppen-Geiger climate regions (Rubel & Kottek (2010)). We show responses of a single crop (rain-fed maize) to applied uniform temperature perturbations, for three discrete precipitation perturbation levels (rain-fed (rf) -20%, rain-fed (0), and rain-fed +20%), with CO₂ and nitrogen held constant at baseline values (360 ppm and 200 kg ha⁻¹ yr⁻¹). Y-axis is fractional change in the regional average climatological potential yield relative to the baseline. The figure shows all modeled land area; see Figure S6 in the supplemental material for only currently-cultivated land. Panel text gives the percentage of rain-fed maize presently cultivated in each climate zone (Portmann et al., 2010). Box-and-whiskers plots show distribution across models, with median marked. Box edges are first and third quartiles, i.e. box height is the interquartile range (IQR). Whiskers extend to maximum and minimum of simulations but are limited at 1.5-IQR; otherwise the outlier is shown. Models generally agree in most climate regions (other than cold continental), with projected changes larger than inter-model variance. Outliers in the tropics (strong negative impact of temperature increases) are the pDSSAT model; outliers in the high-rainfall case (strong positive impact of precipitation increases) are the JULES model. Inter-model variance increases in the case where precipitation is reduced, suggesting uncertainty in model response to water limitation. The right panel with global changes shows yield responses to an globally uniform temperature shift; note that these results are not directly comparable to simulations of more realistic climate scenarios with the same global mean change.

391 parameter estimates towards zero. The Bayesian Ridge method
 392 is necessary to maintain a consistent functional form across all
 393 models, and locations as the linear least squares fails to pro-
 421 vide a stable result in many cases. In the GGCMI Phase II
 422 experiment, the most problematic fits are those for models that
 395 provided a limited number of cases or for low-yield geographic
 423 regions where some modeling groups did not run all scenarios.
 424
 396 Because we do not attempt to emulate models that provided
 425 less than 50 simulations, the lowest number of simulations em-
 400 ulated across the full parameter space is 130 (for the PEPIC
 426 model). We use the implementation of the Bayesian Ridge esti-
 401 mator from the scikit-learn package in Python (Pedregosa et al.,
 427
 402 2011).

403 The resulting parameter matrices for all crop model emula-
 431 tors are available on request, as are the raw simulation data and
 404 a Python application to emulate yields. The yield output for a
 432 single GGCMI model that simulates all scenarios and all five
 406 crops is ~ 12.5 GB; the emulator is ~ 100 MB, a reduction by
 433 over two orders of magnitude.

410 2.4. Emulator evaluation

411 Because no general criteria exist for defining an acceptable
 439 model emulator, we develop a metric of emulator performance
 412 specific to GGCMI. For a multi-model comparison exercise like
 440 GGCMI, a reasonable criterion is what we term the “normalized
 413 error”, which compares the fidelity of an emulator for a given
 441 model and scenario to the inter-model uncertainty. We define
 414 the normalized error e for each scenario as the difference be-
 442 tween the fractional yield change from the emulator and that in
 415 the original simulation, divided by the standard deviation of the
 443 multi-model spread (Equations 2 and 3):

$$F_{scn.} = \frac{Y_{scn.} - Y_{baseline}}{Y_{baseline}}$$

(2)₄₅₀

$$e_{scn.} = \frac{F_{em, scn.} - F_{sim, scn.}}{\sigma_{sim, scn.}} \quad (3)$$

Here $F_{scn.}$ is the fractional change in a model’s mean emulated or simulated yield from a defined baseline, in some scenario (scn.) in C, T, W, and N space; $Y_{scn.}$ and $Y_{baseline}$ are the absolute emulated or simulated mean yields. The normalized error e is the difference between the emulated fractional change in yield and that actually simulated, normalized by $\sigma_{sim.}$, the standard deviation in simulated fractional yields $F_{sim, scn.}$ across all models. The emulator is fit across all available simulation outputs, and then the error is calculated across the simulation scenarios provided by all nine models (Figure 9 and Figures S12 and Figures S13 in supplemental documents). Note that the normalized error e for a model depends not only on the fidelity of its emulator in reproducing a given simulation but on the particular suite of models considered in the intercomparison exercise. The rationale for this choice is to relate the fidelity of the emulation to an estimate of true uncertainty, which we take as the multi-model spread.

438 3. Results

3.1. Simulation results

Crop models in the GGCMI ensemble show a broadly consistent responses to climate and management perturbations in most regions, with a strong negative impact of increased temperature in all but the coldest regions. We illustrate this result for rain-fed maize in Figure 4, which shows yields for the primary Köppen-Geiger climate regions (Rubel & Kottek, 2010). In warming scenarios, models show decreases in maize yield in the temperate, tropical, and arid regions that account for nearly three-quarters of global maize production. These impacts are robust for even moderate climate perturbations. In the temperate zone, even a 1 degree temperature rise with other variables

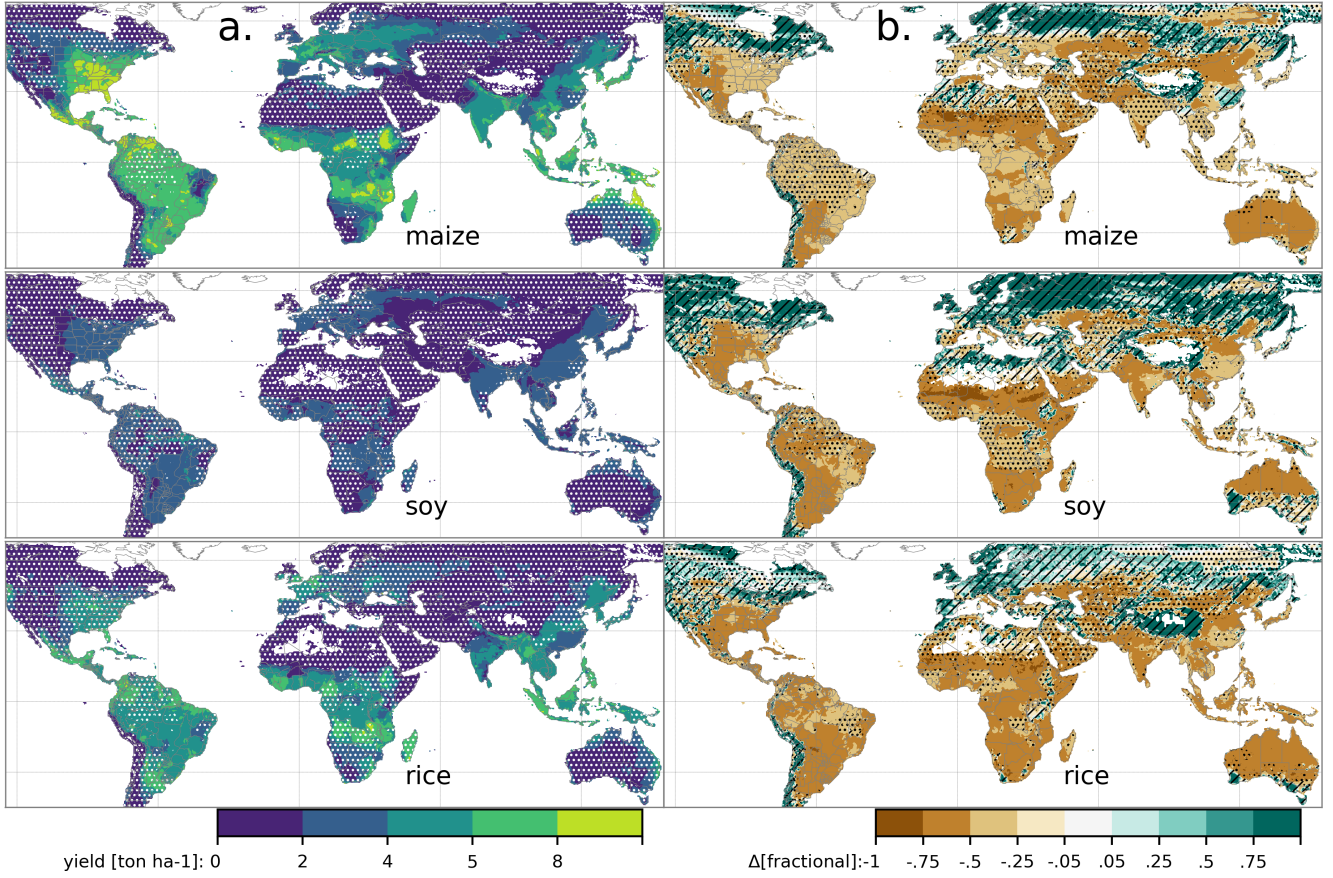


Figure 5: Illustration of the spatial pattern of potential yields and potential yield changes in the GGCMI Phase II ensemble, for three major crops. Left column (a) shows multi-model mean climatological yields for the baseline scenario for (top–bottom) rain-fed maize, soy, and rice. (For wheat see Figure S11 in the supplemental material.) White stippling indicates areas where these crops are not currently cultivated. Absence of cultivation aligns well with the lowest yield contour ($0\text{--}2 \text{ ton ha}^{-1}$). Right column (b) shows the multi-model mean fractional yield change in the extreme $T + 4 \text{ }^{\circ}\text{C}$ scenario (with other inputs at baseline values). Areas without hatching or stippling are those where confidence in projections is high: the multi-model mean fractional change exceeds two standard deviations of the ensemble. ($\Delta > 2\sigma$). Hatching indicates areas of low confidence ($\Delta < 1\sigma$), and stippling areas of medium confidence ($1\sigma < \Delta < 2\sigma$). Crop model results in cold areas, where yield impacts are on average positive, also have the highest uncertainty.

held fixed leads to a median yield reduction that outweighs the variance across models. A 6 degree temperature rise results in median loss of $\sim 25\%$ of yields with a signal to noise of nearly three. A notable exception is the cold continental region, where models disagree strongly, extending even to the sign of impacts. Model simulations of other crops produce similar responses to warming, with robust yield losses in warmer locations and high inter-model variance in the cold continental regions (Figures S7).

The effects of rainfall changes on maize yields are also as expected and are consistent across models. Increased rainfall mitigates the negative effect of higher temperatures, most strongly in arid regions. Decreased rainfall amplifies yield losses and

also increases inter-model variance more strongly, suggesting that models have difficulty representing crop response to water stress. We show only rain-fed maize here; see Figure S5 for the irrigated case. As expected, irrigated crops are more resilient to temperature increases in all regions, especially so where water is limiting.

Mapping the distribution of baseline yields and yield changes shows the geographic dependencies that underlie these results. Figure 5 shows baseline and changes in the $T+4$ scenario for rain-fed maize, soy, and rice in the multi-model ensemble mean, with locations of model agreement marked. Absolute yield potentials are have strong spatial variation, with much of the Earth's surface area unsuitable for any given crop. In general,

models agree most on yield response in regions where yield potentials are currently high and therefore where crops are currently grown. Models show robust decreases in yields at low latitudes, and highly uncertain median increases at most high latitudes. For wheat crops see Figure S11; wheat projections are both more uncertain and show fewer areas of increased yield in the inter-model mean.

3.2. Simulation model validation results

Figure 6 shows the Pearson time series correlation between the simulation model yield and FAO yield data. Figure 6 can be compared to Figures 1,2,3,4 and 6 in Müller et al. (2017). The results are mixed, with many regions for rice and wheat being difficult to model. No single model is dominant, with each model providing near best-in-class performance in at least one location-crop combination. The presence of very few vertical dark green color bars clearly illustrates the power of a multi-model intercomparison project like the one presented here. The ensemble mean does not beat the best model in each case, but shows positive correlation in over 75% of the cases presented here. The EPIC-TAMU model performs best for soy, CARIAB, EPIC-TAMU, and PEPIC perform best for maize, PROMET performs best for wheat, and the EPIC family of models perform best for rice. Reductions in skill over the performance illustrated in Müller et al. (2017) can be attributed to the nitrogen levels or lack of calibration in some models.

*** or harmonization *** Christoph

Soy is qualitatively the easiest crop to represent (except in Argentina), which is likely due in part to the invariance of the response to nitrogen application (soy fixes atmospheric nitrogen very efficiently). Comparison to the FAO data is therefore easier than the other crops because the nitrogen application levels do not matter. US maize has the best performance across models, with nearly every model representing the historical variability to a reasonable extent. Especially good example years for US

maize are 1983, 1988, and 2004 (top left panel of Figure 6), where every model gets the direction of the anomaly compared to surrounding years correct. 1983 and 1988 are famously bad years for US maize along with 2012 (not shown). US maize is possibly both the most uniformly industrialized (in terms of management practices) crop and the one with the best data collection in the historical period of all the cases presented here.

The FAO data is at least one level of abstraction from ground truth in many cases, especially in developing countries. The failure of models to represent the year-to-year variability in rice in some countries in southeast Asia is likely partly due to model failure and partly due to lack of data. It is possible to speculate that the difference in performance between Pakistan (no successful models) and India (many successful models) for rice may reside at least in part in the FAO data and not the models themselves. The same might apply to Bangladesh and India for rice. Partitioning of these contributions is impossible at this stage. Additionally, there is less year-to-year variability in rice yields (partially due to the fraction of irrigated cultivation). Since the Pearson r metric is scale invariant, it will tend to score the rice models more poorly than maize and soy. An example of very poor performance can be seen with the pDSSAT model for rice in India (top right panel of Figure 6).

3.3. Emulator performance

Emulation provides not only a computational tool but a means of understanding and interpreting crop yield response across the parameter space. Emulation is only possible, however, when crop yield responses are sufficiently smooth and continuous to allow fitting with a relatively simple functional form. In the GGCMI simulations, this condition largely but not always holds. Responses are quite diverse across locations, crops, and models, but in most cases local responses are regular enough to permit emulation. Figure 7 illustrates the geographic diversity of responses even in high-yield areas for a

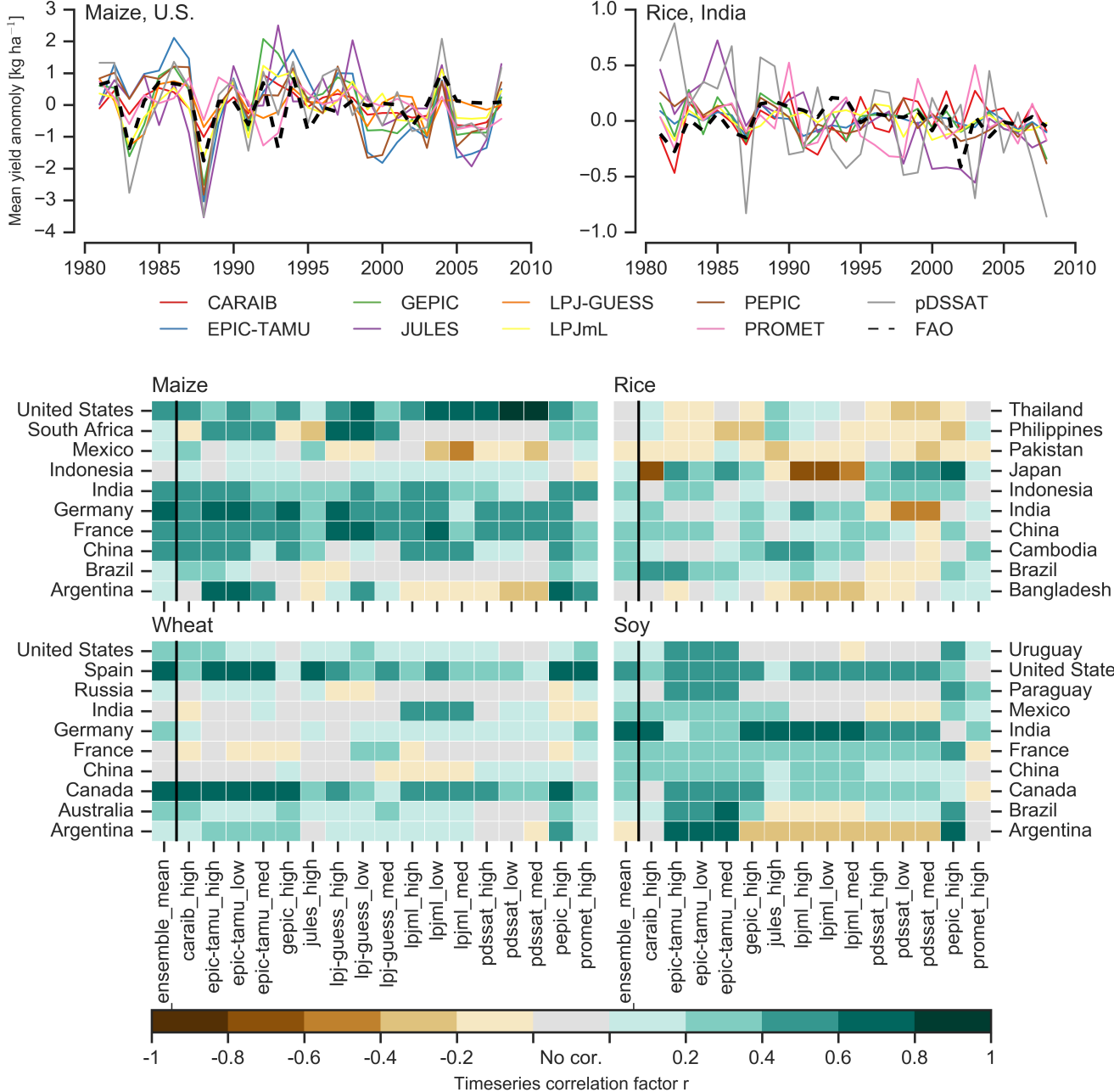


Figure 6: Time series correlation coefficients between simulated crop yield and FAO data (Food and Agriculture Organization of the United Nations, 2018) at the country level. The top panels indicate two example cases: US maize (a good case), and rice in India (mixed case), both for the high nitrogen application case. The heatmaps illustrate the Pearson r correlation coefficient between the detrended simulation mean yield at the country level compared to the detrended FAO yield data for the top producing countries for each crop with continuous FAO data over the 1980-2010 period. Models that provided different nitrogen application levels are shown with low, med, and high label (models that did not simulate different nitrogen levels are analogous to a high nitrogen application level). The ensemble mean yield is also correlated with the FAO data (not the mean of the correlations). Wheat contains both spring wheat and winter wheat simulations.

single crop and model (rain-fed maize in pDSSAT for various high-cultivation areas). This heterogeneity validates the choice of emulating at the grid cell level. Each panel in Figure 7 shows model yield output from scenarios varying only along a single dimension (CO_2 , temperature, precipitation, or nitrogen addition), with other inputs held fixed at baseline levels; in all cases yields evolve smoothly across the space sampled. For reference we show the results of the full emulation fitted across the parameter space. The polynomial fit readily captures the climatological response to

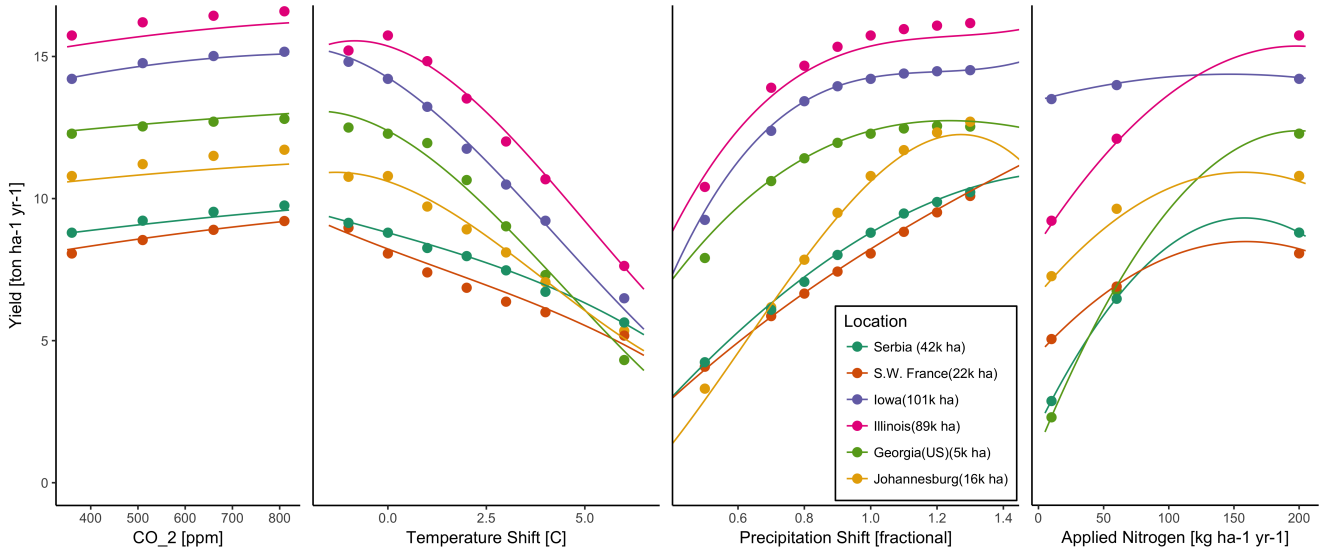


Figure 7: Example illustrating spatial variations in yield response and emulation ability. We show rain-fed maize in the pDSSAT model in six example locations selected to represent high-cultivation areas around the globe. Legend includes hectares cultivated in each selected grid cell. Each panel shows variation along a single variable, with others held at baseline values. Dots show climatological mean yield, solid lines a simple polynomial fit across this 1D variation, and dashed lines the results of the full emulator of Equation 1. The climatological response is sufficiently smooth to be represented by a simple polynomial. Because precipitation changes are imposed as multiplicative factors rather than additive offsets, locations with higher baseline precipitation have a larger absolute spread in inputs sampled than do drier locations (not visible here).

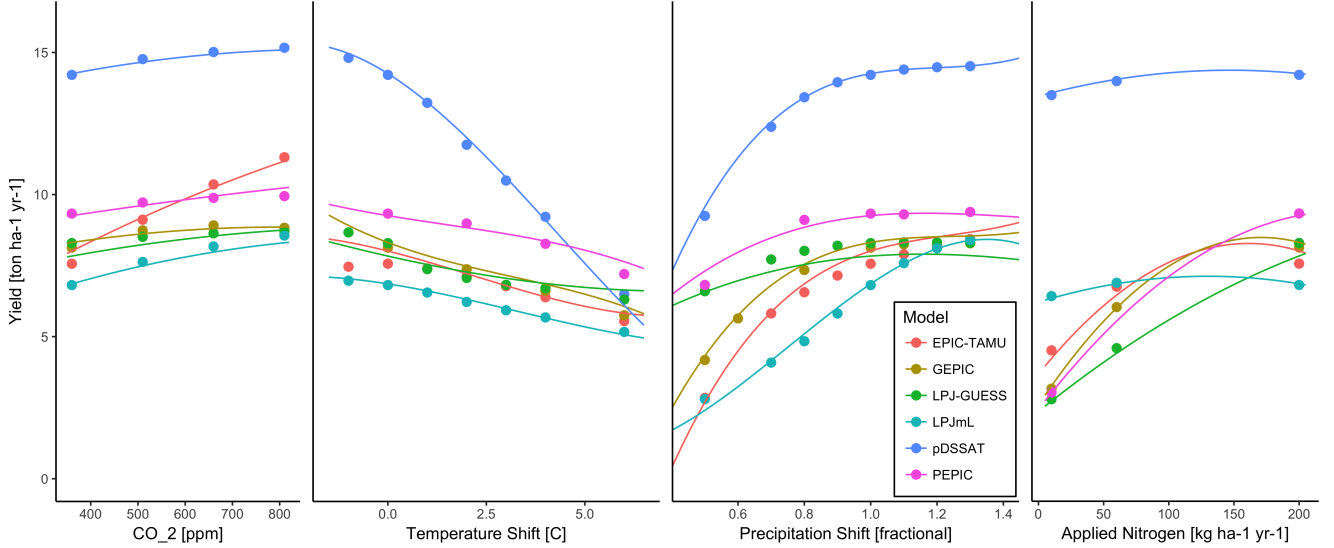


Figure 8: Example illustrating across-model variations in yield response. We show simulations and emulations from six models for rain-fed maize in the same Iowa location shown in Figure 7, with the same plot conventions. Models that did not simulate the nitrogen dimension are omitted for clarity. The inter-model standard deviation is larger for the perturbations in CO₂ and nitrogen than for those in temperature or precipitation illustrating that the sensitivity to weather is better constrained than to management at elevated CO₂. While most model responses can readily be emulated with a simple polynomial, some response surfaces are more complicated and lead to emulation error.

555 perturbations.

560 (rain-fed maize in northern Iowa, the same location shown in
561 the Figure 7). The differences make it important to construct
562 emulators separately for each individual model, and the fidelity
563 of emulation can also differ across models. This figure illus-
564 trates a common phenomenon, that models differ more in re-
565 to the same perturbations, even for a single crop and location

556 Crop yield responses generally follow similar functional
557 forms across models, though with a spread in magnitude. Fig-
558 ure 8 illustrates the inter-model diversity of yield responses
559 to the same perturbations, even for a single crop and location

565 sponse to perturbations in CO₂ and nitrogen perturbations than
 566 to those in temperature or precipitation. (Compare also Figures
 567 4 and S18.) For this location and crop, CO₂ fertilization effects
 568 can range from ~5–50%, and nitrogen responses from nearly
 569 flat to a 60% drop in the lowest-application simulation.

570 While the nitrogen dimension is important and uncertain, it
 571 is also the most problematic to emulate in this work because
 572 of its limited sampling. The GGCMI protocol specified only
 573 three nitrogen levels (10, 60 and 200 kg N y⁻¹ ha⁻¹), so a third-
 574 order fit would be over-determined but a second-order fit can
 575 result in potentially unphysical results. Steep and nonlinear de-
 576 clines in yield with lower nitrogen levels means that some re-
 577 gressions imply a peak in yield between the 100 and 200 kg N
 578 y⁻¹ ha⁻¹ levels. While there may be some reason to believe
 579 over-application of nitrogen at the wrong time in the growing
 580 season could lead to reduced yields, these features are almost
 581 certainly an artifact of under sampling. In addition, the poly-
 582 nomial fit cannot capture the well-documented saturation effect
 583 of nitrogen application (e.g. Ingestad, 1977) as accurately as
 584 would be possible with a non-parametric model.

585 To assess the ability of the polynomial emulation to capture
 586 the behavior of complex process-based models, we evaluate the
 587 normalized emulator error. That is, for each grid cell, model,
 588 and scenario we evaluate the difference between the model yield
 589 and its emulation, normalized by the inter-model standard de-
 590 viation in yield projections. This metric implies that emulation
 591 is generally satisfactory, with several distinct exceptions. Al-
 592 most all model-crop combination emulators have normalized
 593 errors less than one over nearly all currently cultivated hectares
 594 (Figure 9), but some individual model-crop combinations are
 595 problematic (e.g. PROMET for rice and soy, JULES for soy
 596 and winter wheat, Figures S14–S15). Normalized errors for soy
 597 are somewhat higher across all models not because emulator fi-
 598 delity is worse but because models agree more closely on yield

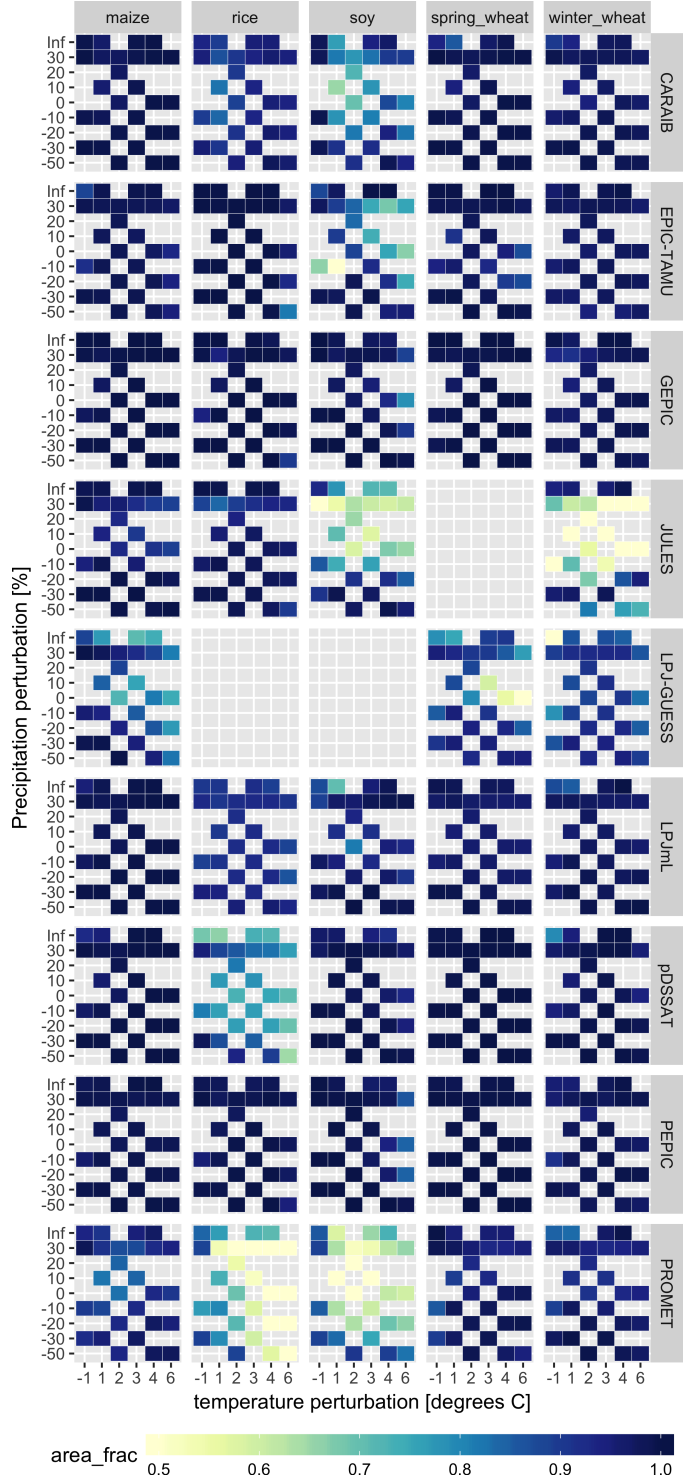


Figure 9: Assessment of emulator performance over currently cultivated areas based on normalized error (Equations 3, 2). We show performance of all 9 models emulated, over all crops and all sampled T and P inputs, but with CO₂ and nitrogen held fixed at baseline values. Large columns are crops and large rows models; squares within are T,P scenario pairs. Colors denote the fraction of currently cultivated hectares with $e < 1$. Of the 756 scenarios with these CO₂ and N values, we consider only those for which all 9 models submitted data. JULES did not simulate spring wheat and LPJ-GUESS did not simulate rice and soy. Emulator performance is generally satisfactory, with some exceptions. Emulator failures (significant areas of poor performance) occur for individual crop-model combinations, with performance generally degrading for hotter and wetter scenarios.

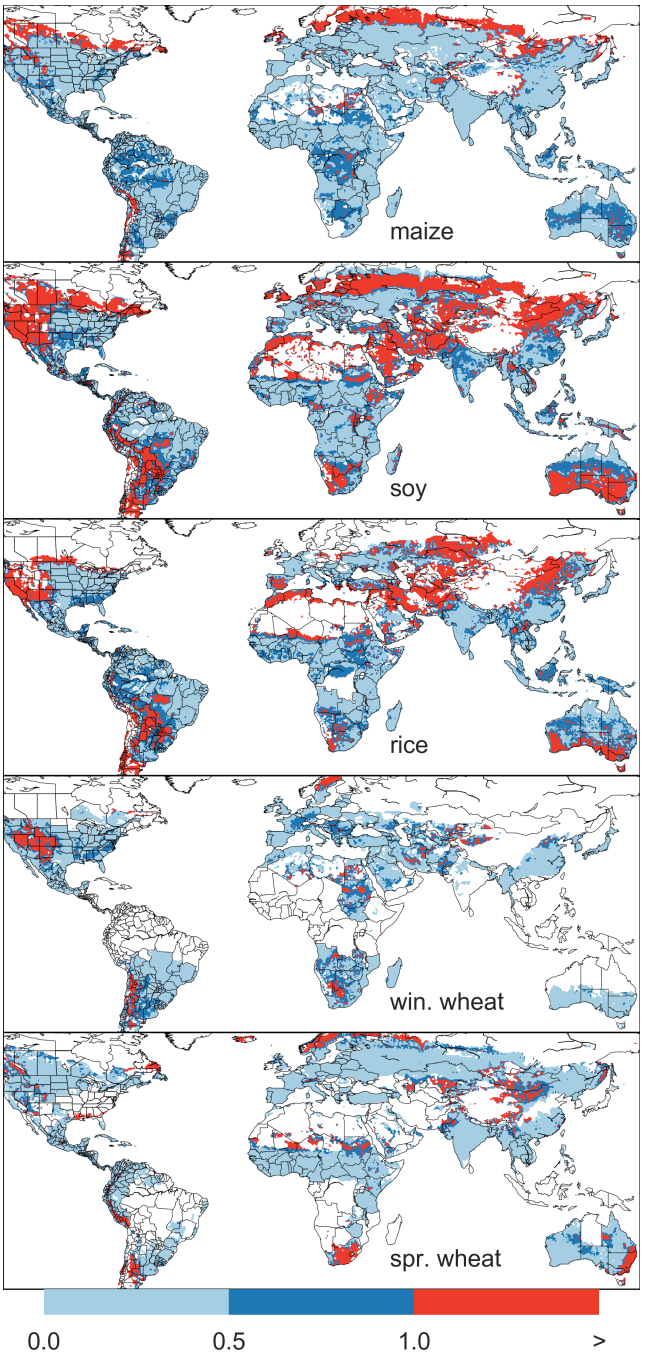


Figure 10: Illustration of our test of emulator performance, applied to the CARAIB model for the T+4 scenario for rain-fed crops. Contour colors indicate the normalized emulator error e , where $e > 1$ means that emulator error exceeds the multi-model standard deviation. White areas are those where crops are not simulated by this model. Models differ in their areas omitted, meaning the number of samples used to calculate the multi-model standard deviation is not spatially consistent in all locations. Emulator performance is generally good relative to model spread in areas where crops are currently cultivated (compare to Figure 1) and in temperate zones in general; emulation issues occur primarily in marginal areas with low yield potentials. For CARAIB, emulation of soy is more problematic, as was also shown in Figure 9.

changes for soy than for other crops (see Figure S16, lowering the denominator. Emulator performance often degrades in geographic locations where crops are not currently cultivated. Figure 10 shows a CARAIB case as an example, where emulator performance is satisfactory over cultivated areas for all crops other than soy, but uncultivated regions show some problematic areas.

It should be noted that this assessment metric is relatively forgiving. First, each emulation is evaluated against the simulation actually used to train the emulator. Had we used a spline interpolation the error would necessarily be zero. Second, the performance metric scales emulator fidelity not by the magnitude of yield changes but by the inter-model spread in those changes. Where models differ more widely, the standard for emulators becomes less stringent. Because models disagree on the magnitude of CO₂ fertilization, this effect is readily seen when comparing assessments of emulator performance in simulations at baseline CO₂ (Figure 9) with those at higher CO₂ levels (Figure S13). Widening the inter-model spread leads to an apparent increase in emulator skill.

3.4. Emulator applications

Because the emulator or “surrogate model” transforms the discrete simulation sample space into a continuous response surface at any geographic scale, it can be used for a variety of applications. Emulators provide an easy way to compare ensembles of climate or impacts projections. They also provide a means for generating continuous damage functions. As an example, we show a damage function constructed from 4D emulations for aggregated yield at the global scale, for maize on currently cultivated land, with simulated values shown for comparison. (Figure 11; see Figures S16- S19 in the supplemental material for other crops and dimensions.) The emulated values closely match simulations even at this aggregation level. Note that these functions are presented only as

examples and do not represent true global projections, because they are developed from simulation data with a uniform temperature shift while increases in global mean temperature should manifest non-uniformly. The global coverage of the GGCMI simulations allows impacts modelers to apply arbitrary geographically-varying climate projections, as well as arbitrary aggregation mask, to develop damage functions for any climate scenario and any geopolitical or geographic level.

across models but evaluation of complex interactions between driving factors (CO_2 , temperature, precipitation, and applied nitrogen) and identification of geographic shifts in high yield potential locations. While the richness of the dataset invites further analysis, we show only a selection of insights derived from the simulations. Across the major crops, inter-model uncertainty is greatest for wheat and least for soy. Across factors impacting yields, inter-model-uncertainty is largest for CO_2 fertilization and nitrogen response effects. Across geographic regions, inter-model uncertainty is largest in the high latitudes where yields may increase, and model projections are most robust in low latitudes where yield impacts are largest.

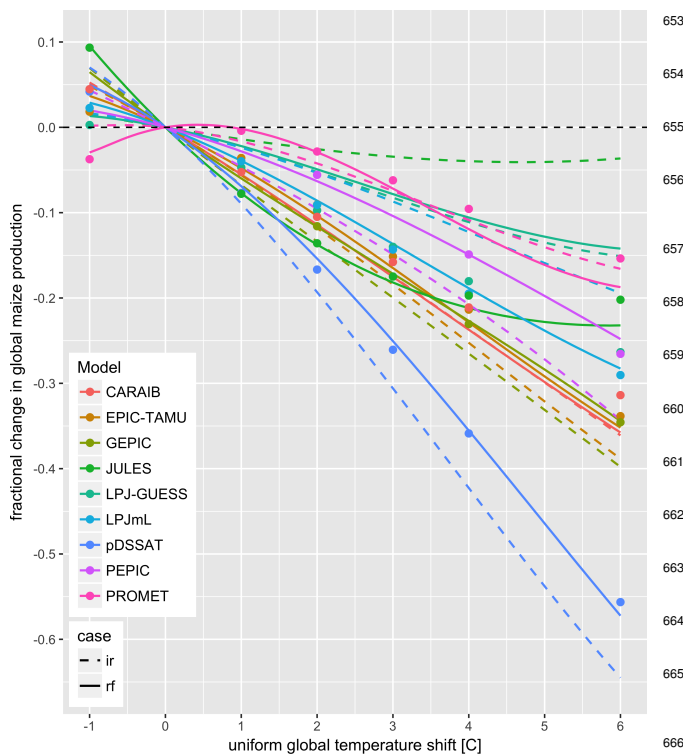


Figure 11: Global emulated damages for maize on currently cultivated lands for the GGCMI models emulated, for uniform temperature shifts with other inputs held at baseline. (The damage function is created from aggregating up-emulated values at the grid cell level, not from a regression of global mean yields.) Lines are emulations for rain-fed (solid) and irrigated (dashed) crops; for comparison, dots are the simulated values for the rain-fed case. For most models, irrigated crops show a sharper reduction than do rain-fed because of the locations of cultivated areas: irrigated crops tend to be grown in warmer areas where impacts are more severe for a given temperature shift. (The exceptions are PROMET, JULES, and LPJmL.) For other crops and scenarios see Figures S16- S19 in the supplemental material.

Model performance when compared to historical data is mixed, with models performing better for maize and soy than for rice and wheat. The value of utilizing multiple models is illustrated by the distribution in performance skill across different countries and crops. An end-user of the simulation outputs or emulator tool may pick and choose models based on historical skill to provide the most faithful temperature and precipitation response depending on their application. The nitrogen and CO_2 responses were not validated in this work.

One counterintuitive result is that irrigated maize shows steeper yield reductions under warming than does rain-fed maize when considered only over currently cultivated land. The effect is the result of geographic differences in cultivated area. In any given location, irrigation increases crop resiliency to temperature increase, but irrigated maize is grown in warmer locations where the impacts of warming are more severe (Figures S5-S6). The same behavior holds for rice and winter wheat, but not for soy or spring wheat (Figures S8-S10). Irrigated wheat and maize are also more sensitive to nitrogen fertilization levels, presumably because growth in rain-fed crops is also water-limited (Figure S19). (Soy as a nitrogen-fixer is relatively insensitive to nitrogen, and rice is not generally grown in water-

4. Conclusions and discussion

The GGCMI Phase II experiment assess sensitivities of process-based crop yield models to changing climate and management inputs, and was designed to allow not only comparison

679 limited conditions).
680 We show that emulation of the output of these complex re-
681 sponds is possible even with a relatively simple reduced-form
682 statistical model and a limited library of simulations. Emula-
683 tion therefore offers the opportunity of producing rapid assess-
684 ments of agricultural impacts for arbitrary climate scenarios in
685 a computationally non-intensive way. The resulting tool should
686 aid in impacts assessment, economic studies, and uncertainty
687 analyses. Emulator parameter values also provide a useful way
688 to compare sensitivities across models to different climate and
689 management inputs, and the terms in the polynomial fits offer
690 the possibility of physical interpretation of these dependencies
691 to some degree.

692 We provide this simulation output dataset for further analysis
693 by the community as we have only scratched the surface with
694 this work. Each simulation run includes year to year variabil-
695 ity in yields under different climate and management regimes.
696 Some of the precipitation and temperature space has been lost
697 due to the aggregation in the time dimension for the emula-
698 tor presented here (i.e. the + 6 C simulation in the hottest year
699 of the historical period compared to the coldest historical year,
700 or precipitation perturbations in the driest historical year etc.).
701 Development of a year-to-year emulator or an emulator at dif-
702 ferent spatial scales may provide useful for some IAM appli-
703 cations. More exhaustive analysis of different statistical model
704 specification for emulation will likely provide additional pre-
705 dictive skill over the specification provided here. The poten-
706 tially richest area for further analysis is the interactions be-
707 tween input variable especially the Nitrogen and CO₂ interac-
708 tions with weather and with each other. More robust quantifica-
709 tion of the sensitivity to the input drivers (and there differences
710 across models), as well as quantification in differences in un-
711 certainty across input drivers. Adaptation via growing season
712 changes were also simulated and are available in the database,
713 though this dimension was not presented or analyzed here. The
output dataset contains many other variables other than yield to
aid in analysis including above ground biomass, LAI, and root
biomass (as many as 25 output variables for some models).

714 The emulation approach presented here has some limitations.
Because the GGCMI simulations apply uniform perturbations
to historical climate inputs, they do not sample changes in
higher order moments. The emulation therefore does not ad-
dress the crop yield impacts of potential changes in climate
variability. While some information could be extracted from
consideration of year-over-year variability, more detailed sim-
ulations and analysis are likely necessary to diagnose the im-
pact of changes in variance and sub-growing-season tempo-
ral effects. Additionally, the emulator is intended to provide
the change in yield from a historical mean baseline value and
should be used in conjunction with historical data (or data prod-
ucts) or a historical mean emulator (not presented here).

715 The future of food security is one of the larger challenges
facing humanity at present. The development (and emulation)
of multi-model ensembles such as GGCMI Phase II provides
a way to begin to quantify uncertainties in crop responses to
a range of potential climate inputs and explore the potential
benefits of adaptive responses. Emulation also allow making
state-of-the-art simulation results available to a wide research
community as simple, computationally tractable tools that can
be used by downstream modelers to understand the socioeco-
nomic impacts of crop response to climate change.

5. Acknowledgments

We thank Michael Stein and Kevin Schwarzwald, who pro-
vided helpful suggestions that contributed to this work. This re-
search was performed as part of the Center for Robust Decision-
Making on Climate and Energy Policy (RDCEP) at the Univer-
sity of Chicago, and was supported through a variety of sources.

746 RDCEP is funded by NSF grant #SES-1463644 through the⁷⁸³
 747 Decision Making Under Uncertainty program. J.F. was sup-⁷⁸⁴
 748 ported by the NSF NRT program, grant #DGE-1735359. C.M.⁷⁸⁵
 749 was supported by the MACMIT project (01LN1317A) funded⁷⁸⁶
 750 through the German Federal Ministry of Education and Re-⁷⁸⁷
 751 search (BMBF). C.F. was supported by the European Research⁷⁸⁸
 752 Council Synergy grant #ERC-2013-SynG-610028 Imbalance-⁷⁸⁹
 753 P. P.F. and K.W. were supported by the Newton Fund through⁷⁹⁰
 754 the Met Office Climate Science for Service Partnership Brazil⁷⁹¹
 755 (CSSP Brazil). A.S. was supported by the Office of Science⁷⁹²
 756 of the U.S. Department of Energy as part of the Multi-sector⁷⁹³
 757 Dynamics Research Program Area. Computing resources were⁷⁹⁴
 758 provided by the University of Chicago Research Computing⁷⁹⁵
 759 Center (RCC). S.O. acknowledges support from the Swedish⁷⁹⁶
 760 strong research areas BECC and MERGE together with sup-⁷⁹⁷
 761 port from LUCCI (Lund University Centre for studies of Car-⁷⁹⁸
 762 bon Cycle and Climate Interactions).⁷⁹⁹

800 Balkovi, J., van der Velde, M., Skalsk, R., Xiong, W., Folberth, C., Khabarov,
 801 N., Smirnov, A., Mueller, N. D., & Obersteiner, M. (2014). Global wheat
 802 production potentials and management flexibility under the representative
 803 concentration pathways. *Global and Planetary Change*, 122, 107 – 121.
 804 Blanc, E. (2017). Statistical emulators of maize, rice, soybean and wheat yields
 805 from global gridded crop models. *Agricultural and Forest Meteorology*, 236,
 806 145 – 161.
 807 Blanc, E., & Sultan, B. (2015). Emulating maize yields from global gridded
 808 crop models using statistical estimates. *Agricultural and Forest Meteorology*, 214-215, 134 – 147.
 809 von Bloh, W., Schaphoff, S., Müller, C., Rolinski, S., Waha, K., & Zaehle, S.
 810 (2018). Implementing the Nitrogen cycle into the dynamic global vegetation,
 811 hydrology and crop growth model LPJmL (version 5.0). *Geoscientific
 812 Model Development*, 11, 2789–2812.
 813 Castruccio, S., McInerney, D. J., Stein, M. L., Liu Crouch, F., Jacob, R. L.,
 814 & Moyer, E. J. (2014). Statistical Emulation of Climate Model Projections
 815 Based on Precomputed GCM Runs. *Journal of Climate*, 27, 1829–1844.
 816 Challinor, A., Watson, J., Lobell, D., Howden, S., Smith, D., & Chhetri, N.
 817 (2014). A meta-analysis of crop yield under climate change and adaptation.
 818 *Nature Climate Change*, 4, 287 – 291.
 819 Conti, S., Gosling, J. P., Oakley, J. E., & O'Hagan, A. (2009). Gaussian process
 820 emulation of dynamic computer codes. *Biometrika*, 96, 663–676.
 821 Duncan, W. (1972). SIMCOT: a simulation of cotton growth and yield. In
 822 C. Murphy (Ed.), *Proceedings of a Workshop for Modeling Tree Growth,*
 823 *Duke University, Durham, North Carolina* (pp. 115–118). Durham, North
 824 Carolina.
 825 Duncan, W., Loomis, R., Williams, W., & Hanau, R. (1967). A model for
 826 simulating photosynthesis in plant communities. *Hilgardia*, (pp. 181–205).
 827 Dury, M., Hambuckers, A., Warnant, P., Henrot, A., Favre, E., Ouberrous,
 828 M., & François, L. (2011). Responses of European forest ecosystems to
 829 21st century climate: assessing changes in interannual variability and fire
 830 intensity. *iForest - Biogeosciences and Forestry*, (pp. 82–99).
 831 Elliott, J., Kelly, D., Chryssanthacopoulos, J., Glotter, M., Jhunjhnuwala, K.,
 832 Best, N., Wilde, M., & Foster, I. (2014). The parallel system for integrating
 833 impact models and sectors (pSIMS). *Environmental Modelling and Soft-
 834 ware*, 62, 509–516.
 835 Elliott, J., Müller, C., Deryng, D., Chryssanthacopoulos, J., Boote, K. J.,
 836 Büchner, M., Foster, I., Glotter, M., Heinke, J., Iizumi, T., Izaurralde, R. C.,
 837 Mueller, N. D., Ray, D. K., Rosenzweig, C., Ruane, A. C., & Sheffield, J.
 838 (2015). The Global Gridded Crop Model Intercomparison: data and mod-
 839 eling protocols for Phase 1 (v1.0). *Geoscientific Model Development*, 8,
 840 261–277.
 841 Eyring, V., Bony, S., Meehl, G. A., Senior, C. A., Stevens, B., Stouffer, R. J.,
 842

763 6. References

- 764 Angulo, C., Ritter, R., Lock, R., Enders, A., Fronzek, S., & Ewert, F. (2013).
 765 Implication of crop model calibration strategies for assessing regional im-⁸⁰⁷
 766 pacts of climate change in europe. *Agric. For. Meteorol.*, 170, 32 – 46.
 767 Asseng, S., Ewert, F., Martre, P., Ritter, R. P., B. Lobell, D., Cammarano, D.,
 768 A. Kimball, B., Ottman, M., W. Wall, G., White, J., Reynolds, M., D. Al-⁸⁰⁸
 769 derman, P., Prasad, P. V. V., Aggarwal, P., Anothai, J., Basso, B., Bier-⁸⁰⁹
 770 nath, C., Challinor, A., De Sanctis, G., & Zhu, Y. (2015). Rising tempera-⁸¹⁰
 771 tures reduce global wheat production. *Nature Climate Change*, 5, 143–147.
 772 doi:10.1038/nclimate2470.⁸¹¹
- 773 Asseng, S., Ewert, F., Rosenzweig, C., Jones, J., Hatfield, J., Ruane, A.,
 774 J. Boote, K., Thorburn, P., Ritter, R. P., Cammarano, D., Brisson, N.,
 775 Basso, B., Martre, P., Aggarwal, P., Angulo, C., Bertuzzi, P., Biernath,
 776 C., Challinor, A., Doltra, J., & Wolf, J. (2013). Uncertainty in simulat-⁸¹²
 777 ing wheat yields under climate change. *Nature Climate Change*, 3, 827832.
 778 doi:10.1038/nclimate1916.⁸¹³
- 779 Aulakh, M. S., & Malhi, S. S. (2005). Interactions of Nitrogen with Other
 780 Nutrients and Water: Effect on Crop Yield and Quality, Nutrient Use Ef-⁸¹⁴
 781 ficiency, Carbon Sequestration, and Environmental Pollution. *Advances in
 782 Agronomy*, 86, 341 – 409.⁸¹⁵
- 800 Balkovi, J., van der Velde, M., Skalsk, R., Xiong, W., Folberth, C., Khabarov,
 801 N., Smirnov, A., Mueller, N. D., & Obersteiner, M. (2014). Global wheat
 802 production potentials and management flexibility under the representative
 803 concentration pathways. *Global and Planetary Change*, 122, 107 – 121.
 804 Blanc, E. (2017). Statistical emulators of maize, rice, soybean and wheat yields
 805 from global gridded crop models. *Agricultural and Forest Meteorology*, 236,
 806 145 – 161.
 807 Blanc, E., & Sultan, B. (2015). Emulating maize yields from global gridded
 808 crop models using statistical estimates. *Agricultural and Forest Meteorology*, 214-215, 134 – 147.
 809 von Bloh, W., Schaphoff, S., Müller, C., Rolinski, S., Waha, K., & Zaehle, S.
 810 (2018). Implementing the Nitrogen cycle into the dynamic global vegetation,
 811 hydrology and crop growth model LPJmL (version 5.0). *Geoscientific
 812 Model Development*, 11, 2789–2812.
 813 Castruccio, S., McInerney, D. J., Stein, M. L., Liu Crouch, F., Jacob, R. L.,
 814 & Moyer, E. J. (2014). Statistical Emulation of Climate Model Projections
 815 Based on Precomputed GCM Runs. *Journal of Climate*, 27, 1829–1844.
 816 Challinor, A., Watson, J., Lobell, D., Howden, S., Smith, D., & Chhetri, N.
 817 (2014). A meta-analysis of crop yield under climate change and adaptation.
 818 *Nature Climate Change*, 4, 287 – 291.
 819 Conti, S., Gosling, J. P., Oakley, J. E., & O'Hagan, A. (2009). Gaussian process
 820 emulation of dynamic computer codes. *Biometrika*, 96, 663–676.
 821 Duncan, W. (1972). SIMCOT: a simulation of cotton growth and yield. In
 822 C. Murphy (Ed.), *Proceedings of a Workshop for Modeling Tree Growth,*
 823 *Duke University, Durham, North Carolina* (pp. 115–118). Durham, North
 824 Carolina.
 825 Duncan, W., Loomis, R., Williams, W., & Hanau, R. (1967). A model for
 826 simulating photosynthesis in plant communities. *Hilgardia*, (pp. 181–205).
 827 Dury, M., Hambuckers, A., Warnant, P., Henrot, A., Favre, E., Ouberrous,
 828 M., & François, L. (2011). Responses of European forest ecosystems to
 829 21st century climate: assessing changes in interannual variability and fire
 830 intensity. *iForest - Biogeosciences and Forestry*, (pp. 82–99).
 831 Elliott, J., Kelly, D., Chryssanthacopoulos, J., Glotter, M., Jhunjhnuwala, K.,
 832 Best, N., Wilde, M., & Foster, I. (2014). The parallel system for integrating
 833 impact models and sectors (pSIMS). *Environmental Modelling and Soft-
 834 ware*, 62, 509–516.
 835 Elliott, J., Müller, C., Deryng, D., Chryssanthacopoulos, J., Boote, K. J.,
 836 Büchner, M., Foster, I., Glotter, M., Heinke, J., Iizumi, T., Izaurralde, R. C.,
 837 Mueller, N. D., Ray, D. K., Rosenzweig, C., Ruane, A. C., & Sheffield, J.
 838 (2015). The Global Gridded Crop Model Intercomparison: data and mod-
 839 eling protocols for Phase 1 (v1.0). *Geoscientific Model Development*, 8,
 840 261–277.
 841 Eyring, V., Bony, S., Meehl, G. A., Senior, C. A., Stevens, B., Stouffer, R. J.,
 842

- & Taylor, K. E. (2016). Overview of the coupled model intercomparison⁸⁶⁹
 project phase 6 (cmip6) experimental design and organization. *Geoscientific⁸⁷⁰*
Model Development, 9, 1937–1958.
- Ferrise, R., Moriondo, M., & Bindi, M. (2011). Probabilistic assessments of cli-⁸⁷²
 mate change impacts on durum wheat in the mediterranean region. *Natural⁸⁷³*
Hazards and Earth System Sciences, 11, 1293–1302.
- Folberth, C., Gaiser, T., Abbaspour, K. C., Schulin, R., & Yang, H. (2012). Re-⁸⁷⁵
 gionalization of a large-scale crop growth model for sub-Saharan Africa:⁸⁷⁶
 Model setup, evaluation, and estimation of maize yields. *Agriculture,⁸⁷⁷*
Ecosystems & Environment, 151, 21 – 33.
- Food and Agriculture Organization of the United Nations (2018). FAOSTAT⁸⁷⁹
 database. URL: <http://www.fao.org/faostat/en/home>.
- Fronzek, S., Pirttioja, N., Carter, T. R., Bindi, M., Hoffmann, H., Palosuo, T.,⁸⁸¹
 Ruiz-Ramos, M., Tao, F., Trnka, M., Acutis, M., Asseng, S., Baranowski, P.,⁸⁸²
 Basso, B., Bodin, P., Buis, S., Cammarano, D., Deligios, P., Destain, M.-F.,⁸⁸³
 Dumont, B., Ewert, F., Ferrise, R., François, L., Gaiser, T., Hlavinka, P.,⁸⁸⁴
 Jacquemin, I., Kersebaum, K. C., Kollas, C., Krzyszczak, J., Lorite, I. J.,⁸⁸⁵
 Minet, J., Minguez, M. I., Montesino, M., Moriondo, M., Müller, C., Nen-⁸⁸⁶
 del, C., Öztürk, I., Perego, A., Rodríguez, A., Ruane, A. C., Ruget, F., Sanna,⁸⁸⁷
 M., Semenov, M. A., Slawinski, C., Stratonovitch, P., Supit, I., Waha, K.,⁸⁸⁸
 Wang, E., Wu, L., Zhao, Z., & Rötter, R. P. (2018). Classifying multi-model⁸⁸⁹
 wheat yield impact response surfaces showing sensitivity to temperature and⁸⁹⁰
 precipitation change. *Agricultural Systems*, 159, 209–224.
- Glotter, M., Elliott, J., McInerney, D., Best, N., Foster, I., & Moyer, E. J. (2014).⁸⁹²
 Evaluating the utility of dynamical downscaling in agricultural impacts pro-⁸⁹³
 jections. *Proceedings of the National Academy of Sciences*, 111, 8776–8781.⁸⁹⁴
- Glotter, M., Moyer, E., Ruane, A., & Elliott, J. (2015). Evaluating the Sensitiv-⁸⁹⁵
 ity of Agricultural Model Performance to Different Climate Inputs. *Journal⁸⁹⁶*
of Applied Meteorology and Climatology, 55, 151113145618001.
- Hank, T., Bach, H., & Mauser, W. (2015). Using a Remote Sensing-Supported⁸⁹⁸
 Hydro-Agroecological Model for Field-Scale Simulation of Heterogeneous⁸⁹⁹
 Crop Growth and Yield: Application for Wheat in Central Europe. *Remote⁹⁰⁰*
Sensing, 7, 3934–3965.
- He, W., Yang, J., Zhou, W., Drury, C., Yang, X., D. Reynolds, W., Wang, H.,⁹⁰²
 He, P., & Li, Z.-T. (2016). Sensitivity analysis of crop yields, soil water⁹⁰³
 contents and nitrogen leaching to precipitation, management practices and⁹⁰⁴
 soil hydraulic properties in semi-arid and humid regions of Canada using the⁹⁰⁵
 DSSAT model. *Nutrient Cycling in Agroecosystems*, 106, 201–215.
- Heady, E. O. (1957). An Econometric Investigation of the Technology of Agri-⁹⁰⁷
 cultural Production Functions. *Econometrica*, 25, 249–268.
- Heady, E. O., & Dillon, J. L. (1961). *Agricultural production functions*. Iowa⁹⁰⁹
 State University Press.
- M., Kanudia, A., & F. B. (2014). Plasim-entsem v1.0: A spatiotemporal
 emulator of future climate change for impacts assessment. *Geoscientific⁹¹⁰*
Model Development, 7, 433–451. doi:10.5194/gmd-7-433-2014.
- Holzkämper, A., Calanca, P., & Fuhrer, J. (2012). Statistical crop models:
 Predicting the effects of temperature and precipitation changes. *Climate⁹¹²*
Research, 51, 11–21.
- Holzworth, D. P., Huth, N. I., deVoil, P. G., Zurcher, E. J., Herrmann, N. I.,⁹¹⁴
 McLean, G., Chenu, K., van Oosterom, E. J., Snow, V., Murphy, C., Moore,⁹¹⁵
 A. D., Brown, H., Whish, J. P., Verrall, S., Fainges, J., Bell, L. W., Peake,⁹¹⁶
 A. S., Poulton, P. L., Hochman, Z., Thorburn, P. J., Gaydon, D. S., Dalgliesh,⁹¹⁷
 N. P., Rodriguez, D., Cox, H., Chapman, S., Doherty, A., Teixeira, E., Sharp,⁹¹⁸
 J., Cichota, R., Vogeler, I., Li, F. Y., Wang, E., Hammer, G. L., Robertson,⁹¹⁹
 M. J., Dimes, J. P., Whitbread, A. M., Hunt, J., van Rees, H., McClelland, T.,⁹²⁰
 Carberry, P. S., Hargreaves, J. N., MacLeod, N., McDonald, C., Harsdorf, J.,⁹²¹
 Wedgwood, S., & Keating, B. A. (2014). APSIM Evolution towards a new
 generation of agricultural systems simulation. *Environmental Modelling and⁹²²*
Software, 62, 327 – 350.
- Howden, S., & Crimp, S. (2005). Assessing dangerous climate change impacts
 on australia's wheat industry. *Modelling and Simulation Society of Australia⁹²⁴*
and New Zealand, (pp. 505–511).
- Iizumi, T., Nishimori, M., & Yokozawa, M. (2010). Diagnostics of climate
 model biases in summer temperature and warm-season insolation for the
 simulation of regional paddy rice yield in japan. *Journal of Applied Meteor-⁹²⁶*
ology and Climatology, 49, 574–591.
- Ingestad, T. (1977). Nitrogen and Plant Growth; Maximum Efficiency of Ni-⁹²⁸
 trogen Fertilizers. *Ambio*, 6, 146–151.
- Izaurrealde, R., Williams, J., McGill, W., Rosenberg, N., & Quiroga Jakas, M.⁹²⁹
 (2006). Simulating soil C dynamics with EPIC: Model description and test-⁹³⁰
 ing against long-term data. *Ecological Modelling*, 192, 362–384.
- Jagtap, S. S., & Jones, J. W. (2002). Adaptation and evaluation of the
 CROPGRO-soybean model to predict regional yield and production. *Agri-⁹³²*
culture, Ecosystems & Environment, 93, 73 – 85.
- Jones, J., Hoogenboom, G., Porter, C., Boote, K., Batchelor, W., Hunt, L.,⁹³⁴
 Wilkens, P., Singh, U., Gijsman, A., & Ritchie, J. (2003). The DSSAT
 cropping system model. *European Journal of Agronomy*, 18, 235 – 265.
- Jones, J. W., Antle, J. M., Basso, B., Boote, K. J., Conant, R. T., Foster, I.,⁹³⁶
 Godfray, H. C. J., Herrero, M., Howitt, R. E., Janssen, S., Keating, B. A.,⁹³⁷
 Munoz-Carpeta, R., Porter, C. H., Rosenzweig, C., & Wheeler, T. R. (2017).⁹³⁸
 Toward a new generation of agricultural system data, models, and knowl-⁹³⁹
 edge products: State of agricultural systems science. *Agricultural Systems*,⁹⁴⁰
 155, 269 – 288.
- Keating, B., Carberry, P., Hammer, G., Probert, M., Robertson, M., Holzworth,⁹⁴¹
 D., Huth, N., Hargreaves, J., Meinke, H., Hochman, Z., McLean, G., Ver-

- burg, K., Snow, V., Dimes, J., Silburn, M., Wang, E., Brown, S., Bristow, K., Asseng, S., Chapman, S., McCown, R., Freebairn, D., & Smith, C. (2003). An overview of APSIM, a model designed for farming systems simulation. *European Journal of Agronomy*, 18, 267 – 288.
- Lindeskog, M., Arneth, A., Bondeau, A., Waha, K., Seaquist, J., Olin, S., & Smith, B. (2013). Implications of accounting for land use in simulations of ecosystem carbon cycling in Africa. *Earth System Dynamics*, 4, 385–407.
- Liu, J., Williams, J. R., Zehnder, A. J., & Yang, H. (2007). GEPIC - modelling wheat yield and crop water productivity with high resolution on a global scale. *Agricultural Systems*, 94, 478 – 493.
- Liu, W., Yang, H., Folberth, C., Wang, X., Luo, Q., & Schulin, R. (2016a). Global investigation of impacts of PET methods on simulating crop-water relations for maize. *Agricultural and Forest Meteorology*, 221, 164 – 175.
- Liu, W., Yang, H., Liu, J., Azevedo, L. B., Wang, X., Xu, Z., Abbaspour, K. C., & Schulin, R. (2016b). Global assessment of nitrogen losses and trade-offs with yields from major crop cultivations. *Science of The Total Environment*, 572, 526 – 537.
- Lobell, D. B., & Burke, M. B. (2010). On the use of statistical models to predict crop yield responses to climate change. *Agricultural and Forest Meteorology*, 150, 1443 – 1452.
- Lobell, D. B., & Field, C. B. (2007). Global scale climate-crop yield relationships and the impacts of recent warming. *Environmental Research Letters*, 2, 014002.
- MacKay, D. (1991). Bayesian Interpolation. *Neural Computation*, 4, 415–447.
- Makowski, D., Asseng, S., Ewert, F., Bassu, S., Durand, J., Martre, P., Adam, M., Aggarwal, P., Angulo, C., Baron, C., Basso, B., Bertuzzi, P., Biernath, C., Boogaard, H., Boote, K., Brisson, N., Cammarano, D., Challinor, A., Conijn, J., & Wolf, J. (2015). Statistical analysis of large simulated yield datasets for studying climate effects. (p. 1100). doi:10.13140/RG.2.1.5173.8328.
- Mauser, W., & Bach, H. (2015). PROMET - Large scale distributed hydrological modelling to study the impact of climate change on the water flows of mountain watersheds. *Journal of Hydrology*, 376, 362 – 377.
- Mauser, W., Klepper, G., Zabel, F., Delzeit, R., Hank, T., Putzenlechner, B., & Calzadilla, A. (2009). Global biomass production potentials exceed expected future demand without the need for cropland expansion. *Nature Communications*, 6.
- McDermid, S., Dilleepkumar, G., Murthy, K., Nedumaran, S., Singh, P., Srinivas, C., Gangwar, B., Subash, N., Ahmad, A., Zubair, L., & Nissanka, S. (2015). Integrated assessments of the impacts of climate change on agriculture: An overview of AgMIP regional research in South Asia. *Chapter in: Handbook of Climate Change and Agroecosystems*, (pp. 201–218).
- Mistry, M. N., Wing, I. S., & De Cian, E. (2017). Simulated vs. empirical weather responsiveness of crop yields: US evidence and implications for the agricultural impacts of climate change. *Environmental Research Letters*, 12.
- Moore, F. C., Baldos, U., Hertel, T., & Diaz, D. (2017). New science of climate change impacts on agriculture implies higher social cost of carbon. *Nature Communications*, 8.
- Müller, C., Elliott, J., Chryssanthacopoulos, J., Arneth, A., Balkovic, J., Ciais, P., Deryng, D., Folberth, C., Glotter, M., Hoek, S., Iizumi, T., Izaurralde, R. C., Jones, C., Khabarov, N., Lawrence, P., Liu, W., Olin, S., Pugh, T. A. M., Ray, D. K., Reddy, A., Rosenzweig, C., Ruane, A. C., Sakurai, G., Schmid, E., Skalsky, R., Song, C. X., Wang, X., de Wit, A., & Yang, H. (2017). Global gridded crop model evaluation: benchmarking, skills, deficiencies and implications. *Geoscientific Model Development*, 10, 1403–1422.
- Nakamura, T., Osaki, M., Koike, T., Hanba, Y. T., Wada, E., & Tadano, T. (1997). Effect of CO₂ enrichment on carbon and nitrogen interaction in wheat and soybean. *Soil Science and Plant Nutrition*, 43, 789–798.
- O'Hagan, A. (2006). Bayesian analysis of computer code outputs: A tutorial. *Reliability Engineering & System Safety*, 91, 1290 – 1300.
- Olin, S., Schurgers, G., Lindeskog, M., Wårliind, D., Smith, B., Bodin, P., Holmér, J., & Arneth, A. (2015). Modelling the response of yields and tissue C:N to changes in atmospheric CO₂ and N management in the main wheat regions of western europe. *Biogeosciences*, 12, 2489–2515. doi:10.5194/bg-12-2489-2015.
- Osaki, M., Shinano, T., & Tadano, T. (1992). Carbon-nitrogen interaction in field crop production. *Soil Science and Plant Nutrition*, 38, 553–564.
- Osborne, T., Gornall, J., Hooker, J., Williams, K., Wiltshire, A., Betts, R., & Wheeler, T. (2015). JULES-crop: a parametrisation of crops in the Joint UK Land Environment Simulator. *Geoscientific Model Development*, 8, 1139–1155.
- Ostberg, S., Schewe, J., Childers, K., & Frieler, K. (2018). Changes in crop yields and their variability at different levels of global warming. *Earth System Dynamics*, 9, 479–496.
- Oyebamiji, O. K., Edwards, N. R., Holden, P. B., Garthwaite, P. H., Schaphoff, S., & Gerten, D. (2015). Emulating global climate change impacts on crop yields. *Statistical Modelling*, 15, 499–525.
- Pedregosa, F., Varoquaux, G., Gramfort, A., Michel, V., Thirion, B., Grisel, O., Blondel, M., Prettenhofer, P., Weiss, R., Dubourg, V., Vanderplas, J., Pas-sos, A., Cournapeau, D., Brucher, M., Perrot, M., & Duchesnay, E. (2011). Scikit-learn: Machine Learning in Python. *Journal of Machine Learning Research*, 12, 2825–2830.
- Pirttioja, N., Carter, T., Fronzek, S., Bindi, M., Hoffmann, H., Palosuo, T., Ruiz-Ramos, M., Tao, F., Trnka, M., Acutis, M., Asseng, S., Baranowski,

- 998 P., Basso, B., Bodin, P., Buis, S., Cammarano, D., Deligios, P., Destain, M.,¹⁰⁴¹
 999 Dumont, B., Ewert, F., Ferrise, R., François, L., Gaiser, T., Hlavinka, P.,¹⁰⁴²
 1000 Jacquemin, I., Kersebaum, K., Kollas, C., Krzyszczak, J., Lorite, I., Minet,¹⁰⁴³
 1001 J., Minguez, M., Montesino, M., Moriondo, M., Müller, C., Nendel, C.,¹⁰⁴⁴
 1002 Öztürk, I., Perego, A., Rodríguez, A., Ruane, A., Ruget, F., Sanna, M.,¹⁰⁴⁵
 1003 Semenov, M., Slawinski, C., Stratovitch, P., Supit, I., Waha, K., Wang,¹⁰⁴⁶
 1004 E., Wu, L., Zhao, Z., & Rötter, R. (2015). Temperature and precipitation¹⁰⁴⁷
 1005 effects on wheat yield across a European transect: a crop model ensemble¹⁰⁴⁸
 1006 analysis using impact response surfaces. *Climate Research*, 65, 87–105.¹⁰⁴⁹
 1007 Porter et al. (IPCC) (2014). Food security and food production systems. Cli¹⁰⁵⁰
 1008 mate Change 2014: Impacts, Adaptation, and Vulnerability. Part A: Global¹⁰⁵¹
 1009 and Sectoral Aspects. Contribution of Working Group II to the Fifth Assess¹⁰⁵²
 1010 ment Report of the Intergovernmental Panel on Climate Change. In C. Fio¹⁰⁵³
 1011 et al. (Ed.), *IPCC Fifth Assessment Report* (pp. 485–533). Cambridge, UK¹⁰⁵⁴
 1012 Cambridge University Press.¹⁰⁵⁵
 1013 Portmann, F., Siebert, S., Bauer, C., & Doell, P. (2008). Global dataset of¹⁰⁵⁶
 1014 monthly growing areas of 26 irrigated crops.¹⁰⁵⁷
 1015 Portmann, F., Siebert, S., & Doell, P. (2010). MIRCA2000 - Global Monthly¹⁰⁵⁸
 1016 Irrigated and Rainfed crop Areas around the Year 2000: A New High¹⁰⁵⁹
 1017 Resolution Data Set for Agricultural and Hydrological Modeling. *Global¹⁰⁶⁰*
1018 Biogeochemical Cycles, 24, GB1011.¹⁰⁶¹
 1019 Pugh, T., Müller, C., Elliott, J., Deryng, D., Folberth, C., Olin, S., Schmid, E.,¹⁰⁶²
 1020 & Arneth, A. (2016). Climate analogues suggest limited potential for inten¹⁰⁶³
 1021 sification of production on current croplands under climate change. *Nature¹⁰⁶⁴*
1022 Communications, 7, 12608.¹⁰⁶⁵
 1023 Räisänen, J., & Ruokolainen, L. (2006). Probabilistic forecasts of near-term cli¹⁰⁶⁶
 1024 mate change based on a resampling ensemble technique. *Tellus A: Dynamic¹⁰⁶⁷*
1025 Meteorology and Oceanography, 58, 461–472.¹⁰⁶⁸
 1026 Ratto, M., Castelletti, A., & Pagano, A. (2012). Emulation techniques for the¹⁰⁶⁹
 1027 reduction and sensitivity analysis of complex environmental models. *Envir¹⁰⁷⁰*
1028 onmental Modelling & Software, 34, 1 – 4.¹⁰⁷¹
 1029 Razavi, S., Tolson, B. A., & Burn, D. H. (2012). Review of surrogate modeling¹⁰⁷²
 1030 in water resources. *Water Resources Research*, 48.¹⁰⁷³
 1031 Roberts, M., Braun, N., R Sinclair, T., B Lobell, D., & Schlenker, W. (2017)¹⁰⁷⁴
 1032 Comparing and combining process-based crop models and statistical models¹⁰⁷⁵
 1033 with some implications for climate change. *Environmental Research Letters¹⁰⁷⁶*
 1034 12.¹⁰⁷⁷
 1035 Rosenzweig, C., Elliott, J., Deryng, D., Ruane, A. C., Müller, C., Arneth, A.,¹⁰⁷⁸
 1036 Boote, K. J., Folberth, C., Glotter, M., Khabarov, N., Neumann, K., Piontek,¹⁰⁷⁹
 1037 F., Pugh, T. A. M., Schmid, E., Stehfest, E., Yang, H., & Jones, J. W. (2014)¹⁰⁸⁰
 1038 Assessing agricultural risks of climate change in the 21st century in a global¹⁰⁸¹
 1039 gridded crop model intercomparison. *Proceedings of the National Academy¹⁰⁸²*
1040 of Sciences, 111, 3268–3273.¹⁰⁸³
 1041 Rosenzweig, C., Jones, J., Hatfield, J., Ruane, A., Boote, K., Thorburn, P.,
 1042 Antle, J., Nelson, G., Porter, C., Janssen, S., Asseng, S., Basso, B., Ew-
 1043 tert, F., Wallach, D., Baigorria, G., & Winter, J. (2013). The Agricultural
 1044 Model Intercomparison and Improvement Project (AgMIP): Protocols and
 1045 pilot studies. *Agricultural and Forest Meteorology*, 170, 166 – 182.
 1046 Rosenzweig, C., Ruane, A. C., Antle, J., Elliott, J., Ashfaq, M., Chatta,
 1047 A. A., Ewert, F., Folberth, C., Hathie, I., Havlik, P., Hoogenboom, G.,
 1048 Lotze-Campen, H., MacCarthy, D. S., Mason-D'Croz, D., Contreras, E. M.,
 1049 Müller, C., Perez-Dominguez, I., Phillips, M., Porter, C., Raymundo, R. M.,
 1050 Sands, R. D., Schleussner, C.-F., Valdivia, R. O., Valin, H., & Wiebe, K.
 1051 (2018). Coordinating AgMIP data and models across global and regional
 1052 scales for 1.5°C and 2.0°C assessments. *Philosophical Transactions of the
 1053 Royal Society of London A: Mathematical, Physical and Engineering Sci-
 1054 ences*, 376.
 1055 Ruane, A. C., Antle, J., Elliott, J., Folberth, C., Hoogenboom, G., Mason-
 1056 D'Croz, D., Müller, C., Porter, C., Phillips, M. M., Raymundo, R. M.,
 1057 Sands, R., Valdivia, R. O., White, J. W., Wiebe, K., & Rosenzweig, C.
 1058 (2018). Biophysical and economic implications for agriculture of +1.5° and
 1059 +2.0°C global warming using AgMIP Coordinated Global and Regional As-
 1060 sessments. *Climate Research*, 76, 17–39.
 1061 Ruane, A. C., Cecil, L. D., Horton, R. M., Gordon, R., McCollum, R., Brown,
 1062 D., Killough, B., Goldberg, R., Greeley, A. P., & Rosenzweig, C. (2013).
 1063 Climate change impact uncertainties for maize in panama: Farm informa-
 1064 tion, climate projections, and yield sensitivities. *Agricultural and Forest
 1065 Meteorology*, 170, 132 – 145.
 1066 Ruane, A. C., Goldberg, R., & Chryssanthacopoulos, J. (2015). Climate forcing
 1067 datasets for agricultural modeling: Merged products for gap-filling and
 1068 historical climate series estimation. *Agric. Forest Meteorol.*, 200, 233–248.
 1069 Ruane, A. C., McDermid, S., Rosenzweig, C., Baigorria, G. A., Jones, J. W.,
 1070 Romero, C. C., & Cecil, L. D. (2014). Carbon-temperature-water change
 1071 analysis for peanut production under climate change: A prototype for the
 1072 agmip coordinated climate-crop modeling project (c3mp). *Glob. Change
 1073 Biol.*, 20, 394–407. doi:10.1111/gcb.12412.
 1074 Rubel, F., & Kottek, M. (2010). Observed and projected climate shifts 1901–
 1075 2100 depicted by world maps of the Köppen-Geiger climate classification.
Meteorologische Zeitschrift, 19, 135–141.
 1076 Sacks, W. J., Deryng, D., Foley, J. A., & Ramankutty, N. (2010). Crop planting
 1077 dates: an analysis of global patterns. *Global Ecology and Biogeography*, 19,
 1078 607–620.
 1079 Schauberger, B., Archontoulis, S., Arneth, A., Balkovic, J., Ciais, P., Deryng,
 1080 D., Elliott, J., Folberth, C., Khabarov, N., Müller, C., A. M. Pugh, T., Rolin-
 1081 sksi, S., Schaphoff, S., Schmid, E., Wang, X., Schlenker, W., & Frieler, K.
 1082 (2017). Consistent negative response of US crops to high temperatures in

- 1084 observations and crop models. *Nature Communications*, 8, 13931. 1127
- 1085 Schlenker, W., & Roberts, M. J. (2009). Nonlinear temperature effects indicate 128
1086 severe damages to U.S. crop yields under climate change. *Proceedings of the National Academy of Sciences*, 106, 15594–15598. 129
- 1087
- 1088 Snyder, A., Calvin, K. V., Phillips, M., & Ruane, A. C. (2018). A crop yield 1089
1090 change emulator for use in gcam and similar models: Persephone v1.0. *Geoscientific Model Development Discussions*, 2018, 1–42.
- 1091 Storlie, C. B., Swiler, L. P., Helton, J. C., & Sallaberry, C. J. (2009). Implementation 1092
1093 and evaluation of nonparametric regression procedures for sensitivity analysis of computationally demanding models. *Reliability Engineering & System Safety*, 94, 1735 – 1763.
- 1094
- 1095 Taylor, K. E., Stouffer, R. J., & Meehl, G. A. (2012). An overview of CMIP5 1096
1097 and the experiment design. *Bulletin of the American Meteorological Society*, 93, 485–498.
- 1098 Tebaldi, C., & Lobell, D. B. (2008). Towards probabilistic projections of climate 1099
1100 change impacts on global crop yields. *Geophysical Research Letters*, 35.
- 1101 Valade, A., Ciais, P., Vuichard, N., Viovy, N., Caubel, A., Huth, N., Marin, F., & Martin, J. F. (2014). Modeling sugarcane yield with a process-based model from site to continental scale: Uncertainties arising from model structure and parameter values. *Geoscientific Model Development*, 7, 1225–1245.
- 1102
- 1103 Warszawski, L., Frieler, K., Huber, V., Piontek, F., Serdeczny, O., & Schewe, J. (2014). The Inter-Sectoral Impact Model Intercomparison Project (ISI-MIP): Project framework. *Proceedings of the National Academy of Sciences*, 111, 3228–3232.
- 1104
- 1105 White, J. W., Hoogenboom, G., Kimball, B. A., & Wall, G. W. (2011). Methodologies 1106
1107 for simulating impacts of climate change on crop production. *Field Crops Research*, 124, 357 – 368.
- 1108
- 1109 Williams, K., Gornall, J., Harper, A., Wiltshire, A., Hemming, D., Quaife, T., Arkebauer, T., & Scoby, D. (2017). Evaluation of JULES-crop performance 1110
1111 against site observations of irrigated maize from Mead, Nebraska. *Geoscientific Model Development*, 10, 1291–1320.
- 1112
- 1113 Williams, K. E., & Falloon, P. D. (2015). Sources of interannual yield variability 1114
1115 in JULES-crop and implications for forcing with seasonal weather forecasts. *Geoscientific Model Development*, 8, 3987–3997.
- 1116
- 1117 de Wit, C. (1957). Transpiration and crop yields. *Verslagen van Landbouwkundige Onderzoeken* : 64.6, .
- 1118
- 1119 Wolf, J., & Oijen, M. (2002). Modelling the dependence of european potato 1120
1121 yields on changes in climate and co2. *Agricultural and Forest Meteorology*, 112, 217 – 231.
- 1122
- 1123 Zhao, C., Liu, B., Piao, S., Wang, X., Lobell, D. B., Huang, Y., Huang, M., Yao, Y., Bassu, S., Ciais, P., Durand, J. L., Elliott, J., Ewert, F., Janssens, I. A., Li, T., Lin, E., Liu, Q., Martre, P., Miller, C., Peng, S., Peuelas, J., Ruane,